Naval Surface Warfare Center
Carderock Division
West Bethesda, MD 20817-5700

NSWCCD-70-TR–2001/055 April 2001

Signatures Directorate

Research and Development Report

Dependence of the Induced Loss Factor on the Coupling Forms and Coupling Strengths: Linear Analysis

by

G. Maidanik and K. J. Becker

NSWCCD-70-TR–2001/055

REPORT DOCUMENTATION PAGE

Form Approved OMB No. 0704-0188

1. REPORT DATE *(DD-MM-YYYY)*	2. REPORT TYPE	3. DATES COVERED *(From - To)*
20-Apr-2001	Final	-

4. TITLE AND SUBTITLE

Dependence of the Induced Loss Factor on the Coupling Forms and Coupling Strengths: Linear Analysis

5a. CONTRACT NUMBER

5b. GRANT NUMBER

5c. PROGRAM ELEMENT NUMBER

6. AUTHOR(S)

G. Maidanik and K. J. Becker

5d. PROJECT NUMBER

5e. TASK NUMBER

5f. WORK UNIT NUMBER

7. PERFORMING ORGANIZATION NAME(S) AND ADDRESS(ES) AND ADDRESS(ES)

Naval Surface Warfare Center
Carderock Division
9500 Macarthur Boulevard
West Bethesda, MD 20817-5700

8. PERFORMING ORGANIZATION REPORT NUMBER

NSWCCD-70-TR-2001/055

9. SPONSORING / MONITORING AGENCY NAME(S) AND ADDRESS(ES)

10. SPONSOR/MONITOR'S ACRONYM(S)

11. SPONSOR/MONITOR'S REPORT NUMBER(S)

12. DISTRIBUTION / AVAILABILITY STATEMENT

Approved for public release; Distribution is unlimited.

13. SUPPLEMENTARY NOTES

14. ABSTRACT

The influence of a set of satellite oscillators on the response behavior of a master oscillator, to which the set is coupled, is of fundamental significance to structural acoustics and beyond. The focus is largely on the induced loss factor that the satellite oscillators generate in the impedance of the master oscillator. Much of the research work performed on behalf of this investigation employed basically sprung-masses for the satellite oscillators. A sprung-mass is a primitive type of satellite oscillator and, as such, limitations are imposed on the range of applicability of these research works. In this paper more elaborate satellite oscillators are introduced; and, especially, a wider range of coupling forms and strengths are investigated. A number of new insights are, thereby, obtained. In particular, this paper is to facilitate further studies of the relationships among the linear impedance (LIA), the energy analysis (EA) and the statistical energy analysis (SEA). These studies are in progress and are to be reported subsequently.

15. SUBJECT TERMS

16. SECURITY CLASSIFICATION OF:			17. LIMITATION OF ABSTRACT	18. NUMBER OF PAGES	19a. NAME OF RESPONSIBLE PERSON
a. REPORT	b. ABSTRACT	c. THIS PAGE			G. Maidanik
UNCLASSIFIED	UNCLASSIFIED	UNCLASSIFIED	SAR	0	19b. TELEPHONE NUMBER *(include area code)* 301-227-1292

Contents

Dependence of the Induced Loss Factor on the Coupling Forms and Coupling Strengths: Linear Analysis

G. Maidanik and K. J. Becker

Naval Surface Warfare Center, Carderock Division

9500 MacArthur Boulevard

West Bethesda, MD 20817

Abstract

The influence of a set of satellite oscillators on the response behavior of a master oscillator, to which the set is coupled, is of fundamental significance to structural acoustics and beyond. The focus is largely on the induced loss factor that the satellite oscillators generate in the impedance of the master oscillator. Much of the research work performed on behalf of this investigation employed basically sprung-masses for the satellite oscillators. A sprung-mass is a primitive type of satellite oscillator and, as such, limitations are imposed on the range of applicability of these research works. In this paper more elaborate satellite oscillators are introduced; and, especially, a wider range of coupling forms and strengths are investigated. A number of new insights are, thereby, obtained. In particular, this paper is to facilitate further studies of the relationships among the linear impedance analysis (LIA), the energy analysis (EA) and the statistical energy analysis (SEA). These studies are in progress and are to be reported subsequently.

I. Introduction

In a companion paper, designated as Reference 1, the complex is specified in terms of the impedance $Z_o^o(\omega)$ of the isolated master oscillator, the impedance $(i\omega m_r)$ of the (r)th isolated satellite "oscillator" and the coupling impedance $(k_r / i\omega)$; the coupling is between the master oscillator and the satellite oscillator. This complex is sketched in Fig.1a [2-11]. In this complex, the satellite oscillators remain uncoupled to each other. The purpose in the present paper is to introduce a significant extension in scope. In this extension the isolated master oscillator remains the same. An isolated satellite oscillator, the (r)th, is specified by the impedance $Z_r(\omega)$ that may consist of both a mass and a stiffness control term. The coupling of this satellite oscillator to the master oscillator is specified by the coupling impedance $Z_{cr}(\omega)$ and a gyroscopic coupling coefficient (G_r) [12,13]. The coupling impedance $Z_{cr}(\omega)$ consists of a mass and a stiffness control term. A complex of this type is sketched in Fig. 1b. The mass and the stiffness control terms in this complex are related in the forms

$$K = K_o(1+i\eta_o) \quad ; \qquad (K_o / M) = \omega_o^2 , \tag{1a}$$

$$k_r = k_{or}(1+i\eta_r) \quad ; \qquad (k_{or} / m_r) = \omega_r^2 , \tag{1b}$$

$$k_{cr} = k_{ocr}(1+i\eta_{cr}) \quad ; \qquad (k_{ocr} / m_r) = \omega_{cr}^2 , \tag{1c}$$

where the pairs $\{M,K\}$, $\{m_r,k_r\}$, and $\{m_r,k_{cr}\}$ are, respectively, in reference to the master oscillator, to the (r)th satellite oscillator and to the coupling between them. The parameters (η_o), (η_r), and (η_{cr}) are the corresponding stiffness control loss factors, respectively. To complete the definition of the coupling, the mass (m_{cr}) and the gyroscopic coefficient (G_r) need to be specified [12, 13]. These are specified through the coupling parameters which are defined in the normalized forms

$$\bar{m}_{cr} = (m_{cr}/m_r)\ ; \qquad \bar{g}_r = [G_r/(\omega_o m_r)]\,, \tag{1d}$$

respectively. With the assistance of Fig. 1b, the linear equations of motion of the master oscillator in situ and of a typical satellite oscillator in situ are derived

$$Z_o^o(\omega)V_o(\omega)+\sum_1^R Z_{cr}(\omega)\,V_o(\omega) + [Z_{cr}^-(\omega) - G_r]V_r(\omega) = P_e(\omega), \tag{2a}$$

$$[Z_r(\omega)+Z_{cr}(\omega)]V_r(\omega) + [Z_{cr}^-(\omega)+G_r]V_o(\omega) = 0\,, \tag{2b}$$

respectively, where $V_o(\omega)$ and $V_r(\omega)$ are the responses of the mass (M) of the master oscillator and the mass (m_r) of the (r)th satellite oscillator, respectively, (R) is the number of satellite oscillators that are coupled to the master oscillator, $P_e(\omega)$ is the drive that is applied externally to the master oscillator; the satellite oscillators are not driven externally, $Z_o^o(\omega)$ is the impedance of the master oscillator in isolation

$$Z_o^o(\omega) = (i\omega M)[1-(y)^{-2}(1+i\eta_o)]; \qquad y = (\omega/\omega_o), \tag{3a}$$

$Z_r(\omega)$ is the impedance of the (r) th satellite oscillator in isolation

$$Z_r(\omega) = (i\omega m_r)[1-(z_r)^2(1+i\eta_r)]; \quad x_r = (\omega_r/\omega_o); \quad z_r = (x_r/y), \tag{3b}$$

$Z_{cr}(\omega)$ is the impedance of the coupling between the master oscillator and the (r) th satellite oscillator

$$Z_{cr}(\omega) = (i\omega m_r)[\bar{m}_{cr}-(z_{cr})^2(1+i\eta_{cr})];$$

$$\bar{m}_{cr} = (m_{cr}/m_r); \quad x_{cr} = (\omega_{cr}/\omega_o); \quad z_{cr} = (x_{cr}/y), \tag{3c}$$

$Z_{cr}^-(\omega)$ is an impedance that is related to the coupling impedance $Z_{cr}(\omega)$; namely

$$Z_{cr}^-(\omega) = (i\omega m_r)[\bar{m}_{cr}+(z_{cr})^2(1+i\eta_{cr})], \tag{3d}$$

and $(\bar{m}_{cr}), (x_{cr}), (\eta_{cr})$, and (G_r) are defined in Eqs. (1) and (2) [12]. The superscript (o) is reserved to designate quantities that pertain either to the master oscillator in isolation or to satellite oscillators under certain and definitive impositions. Thus, for example, from Eqs. (2a) and (3a), one may state

$$Z_o^o(\omega)V_o^o(\omega) = P_e(\omega), \tag{4}$$

where $V_o^o(\omega)$ is the response of the master oscillator in isolation. By a straightforward algebraic manipulation of Eq. (2) one derives

$$Z_o(\omega)\,V_o(\omega) = P_e(\omega); \qquad V_r(\omega) = B_r(\omega)V_o(\omega), \tag{5}$$

where

$$Z_o(\omega) = Z_o^o(\omega) + \sum_1^R [\{Z_r(\omega) Z_{cr}(\omega)\} + (Q_{cr})^2] [Z_r(\omega) + Z_{cr}(\omega)]^{-1}, \qquad (6a)$$

$$B_r(\omega) = [Z_{cr}^-(\omega) + G_r][Z_r(\omega) + Z_{cr}(\omega)]^{-1}, \qquad (6b)$$

$$(Q_{cr})^2 = 4 m_{cr} k_{cr} + (G_r)^2, \qquad (6c)$$

and the quantities $Z_o^o(\omega)$, $Z_r(\omega)$, $Z_{cr}(\omega)$ and $Z_{cr}^-(\omega)$ are stated explicitly in Eq. (3). Indeed, from Eqs. (1), (3) and (6) one obtains

$$Z_o(\omega) = Z_o(y) = (i\omega M)[1 - (y)^{-2} \{[1 - S(y)] + i[\eta_o + \eta_s(y)]\}], \qquad (7a)$$

$$B_r(\omega) = -[\bar{m}_{cr} + (z_{cr})^2 (1 + i\eta_{cr}) - i(\bar{g}_r / y)] \cdot$$

$$[(1 + \bar{m}_{cr}) - (z_{rr})^2 (1 + i\eta_{rr})]^{-1}, \qquad (7b)$$

where

$$(x_{rr})^2 (1 + i\eta_{rr}) = (x_r)^2 (1 + i\eta_{cr}) + (x_{cr})^2 (1 + i\eta_{cr}), \qquad (8a)$$

$$[S(y) - i\eta_s(y)] = (y)^2 \sum_1^R \{\bar{m}_r \{[1 - (z_r)^2 (1 + i\eta_r)] \cdot$$

$$[\bar{m}_{cr} - (z_{cr})^2 (1 + i\eta_{cr})] - (\bar{q}_{cr} / y)^2\} \cdot$$

$$[(1 + \bar{m}_{cr}) - (z_{rr})^2 (1 + i\eta_{rr})]^{-1}\} \qquad (8b)$$

and, again

$$z_{rr} = (x_{rr} / y)\,; \qquad z_r = (x_r / y)\,; \qquad z_{cr} = (x_{cr} / y)\,;$$

$$(\bar{q}_{cr} / y)^2 = 4\,\bar{m}_{cr}\,(z_{cr})^2\,(1 + i\eta_{cr}) + (\bar{g}_r / y)^2\,; \qquad \bar{q}_{cr} = [Q_{cr} / (\omega_o\, m_r)]. \qquad (8c)$$

One notes that the compound coupling parameter $(\bar{q}_{cr})$ is a functional of the mass and gyroscopic coupling parameters $(\bar{m}_{cr})$ and $(\bar{g}_r)$, respectively. These coupling parameters are defined in Eq. (1d). One also notes, with satisfaction, that the dependence of the terms in the sum on the gyroscopic coupling parameter $(\bar{g}_r)$ is quadratic so that the sign assigned to the gyroscopic coefficient (G_r) plays no role in the influence of the individual satellite oscillators on the impedance of the master oscillator. The gyroscopic coupling is in quadrature to both, the mass and the stiffness control couplings.

Examination of Eqs. (7) and (8) shows that the normalized impedance that the satellite oscillators collectively induce on the master oscillator may be cast in term of the two-vector $\{S(y), \eta_s(y)\}(R)$, which is a function of (R), as indicated. The evaluation of this two-vector, however, is predicated on explicitly specifying the two-vector $\{x_{rr}, \eta_{rr}\}(R)$, its two supplemental components $\{x_r, \eta_r\}(R)$ and $\{x_{cr}, \eta_{cr}\}(R)$ and finally assigning the compound coupling $(\bar{q}_{cr})$. The two-vector $\{x_{rr}, \eta_{rr}\}(R)$ is designed, for the sake of convenience, to stay fixed with respect to variations in the index (r). In this design, the springs, that are placed on either side of the mass of a satellite oscillator, are set to be

similar. With this design, Eq. (8b) is evaluated. In this paper the induced reactive factor $S(y)$ is not considered, here the prime interest is focused on the induced loss factor $\eta_s(y)$. The induced loss factor $\eta_s(y)$ is examined for a variety of coupling forms and coupling strengths as well as for a number of values of the modal overlap parameters (b_r) and (b_{cr}) associated with the loss factors η_r and η_{cr}, respectively [1]. By and large, (b_r) is set equal to (b_{cr}) and they are equated to (b); $b = b_r = b_{cr}$. The simplifying equalities are imposed without considerable loss in generality. Using Eq. (8b), the exact evaluations of $\eta_s(y)$ are executed for three values of (b); $b = (0.1), (2.0)$ and (10). In these evaluations one finds that $\eta_s(y)$ is a function (b). On the other hand, the first order approximation of $\eta_s(y)$, designated by $\eta_I(y)$, that is derived from the replacement of the summation in Eq. (8b) by an integration, is found to be independent of (b). The evaluations are graphically displayed; three exact evaluations for the three values of (b) and the corresponding first order approximation of $\eta_s(y)$ are superimposed in each of the displays. The comparison between these four evaluations can thus be made at a glance, assisting greatly in the interpretation of the data that is computed and displayed. In the frequency range of concern, when (b) is small compared with unity the levels in the exact evaluations of $\eta_s(y)$ undulate, as a function of (y). (The frequency range of concern spans the resonance frequencies of the satellite oscillators.) The excursions in the undulations increase with decrease in (b). It is argued

that the first order approximation constitutes the mean-value averaging of the undulated levels of $\eta_s(y)$ when (b) is small compared with unity and, again, this mean-value curve is independent of (b) [1, 14]. As (b) approaches and increases above unity the undulations in the exact levels of $\eta_s(y)$ are suppressed and the phenomenon of erosion commences and increases. In the frequency range of concern, for these increasing values of (b), erosions are manifested by progressive decreases of the levels, in the exact evaluations of $\eta_s(y)$, from the levels of the corresponding first order approximation [2, 3].

II. Resonance Frequency Distribution of and Assignment of Individual Loss Factors to the Satellite Oscillators

It has been argued that the coupling between two oscillators may cause a shift in the resonance frequency that each has in isolation. Indeed, it was suggested that this shift may be used to determine the "coupling strength" [15, 16]. One may then question as to what exactly are these shifts and are they significant. The shifts, as such, and the implications that they may harbor are not addressed in the present paper; here these shifts are overridden by design. The design intends to derive a suitable resonance frequency distribution and a proper assignment of individual loss factors to the satellite oscillators. The design is expressed, then, in terms of the two-vector $\{x_{rr}, \eta_{rr}\}(R)$, where (x_{rr}) is the normalized resonance frequency and (η_{rr}) is the loss factor associated with the (r)th satellite oscillator. Examination of Eqs. (7) and (8) shows that the normalized resonance frequencies of the satellite oscillators, in situ, are ascertained by satisfying the equality

$$(1 + \bar{m}_c)(y)^2 = (x_{rr})^2; \quad (1 + \bar{m}_c) = (z_{rr})^2; \quad (x_{rr})^2 = (x_r)^2 + (x_{cr})^2. \qquad (9a)$$

As in Reference 1, here too (x_{rr}) is assigned a priori with equal numbers of resonance frequencies on either side of the resonance frequency (ω_o) of the

master oscillator and the distribution is aligned in ascending order; namely

$$x_{rr} \leq x_{qq}\ ; \qquad q = (r+1)\ ; \qquad 1 \leq r \leq (R-1). \tag{9b}$$

A scheme that simultaneously satisfies Eqs. (9a) and (9b) and the mid-point just imposed, demands a supplemental condition of design between the two spring stiffnesses that support the mass of a satellite oscillator. [cf. Fig 1b.] This condition of design requires that

$$(x_{rr})^2 = (1 + \overline{m}_{cr}) \quad \text{for} \quad \overline{r} = (1/2)\,, \tag{9c}$$

where, in Eq. (9c), $(\overline{r})$ may be allowed a continuous connotation [1]. Consulting Reference 1 and using Eq. (9a), one may express the loss factors that are associated with the (r) th satellite oscillator in the forms

$$\eta_r = [b_r / 2(x_r)^2]\, \partial (x_r)^2 / \partial r]\ ; \qquad \eta_{cr} = [b_{cr} / 2(x_{cr})^2][\partial (x_{cr})^2 / \partial r]\ ;$$

$$\eta_{rr} = [(x_{rr})^2 \Gamma^{-1}\ \{(x_r)^2\ \eta_r + (x_{cr})^2\, \eta_{cr}\}, \tag{10}$$

where (b_r) and (b_{cr}) are the modal overlap parameters assigned to the back spring and the fore spring. These two springs support the mass (m_r). [cf. Fig. 1b.] For the sake of simplicity and computational advantage, the stiffness on either side of the mass of a satellite oscillator are assumed to be "similar" in the sense

$$(x_r) = (\alpha_r)^{1/2}\, (x_r^o);\ \ (x_{cr}) = (\alpha_{cr})^{1/2}\ (x_r^o);\ \ (x_{rr}) = (\alpha_r + \alpha_{cr})^{1/2}\, (x_r^o), \tag{11}$$

where (α_r) and (α_{cr}) are dubbed the spring factors. In keeping with the definitions of $(\overline{m}_{cr})$ and $(\overline{g}_r)$, as the mass coupling parameter and the gyroscopic

coupling parameter, the spring factor (α_{cr}) may be designated the stiffness coupling parameter. It is conducive to specify (x_r^o) in a form that is compatible with one of the forms introduced in Reference 1; namely

$$x_r^o = [1+\{1-2\bar{r}\}\,\gamma(\bar{R})]^{-1/2}, \tag{12}$$

where

$$\bar{r} = r(R+1)^{-1}; \quad \bar{R} = R(R+1)^{-1}; \quad \gamma(\bar{R}) = [\gamma/(2\bar{R})]; \quad \gamma<1, \tag{13}$$

and (r) may be discrete; $1 \le r \le R$, or continuous $(\varepsilon) < r < (R+\varepsilon)$ with $\varepsilon < 1$. It should be appreciated, however, that although in this paper Eq. (12) is cast in stone, other forms for (x_r^o) may be readily introduced and similarly manipulated. Also and similarly, as introduced in Reference 1, the normalized mass $(\bar{m}_r)$ of the (r)th satellite oscillator is assumed to be independent of (r) and to be of the form

$$\bar{m}_r = (m_r/M) = (M_s/M)(R)^{-1}; \quad M_s = \sum_1^R (m_r). \tag{14}$$

With the intended exceptions of the last section in this paper it is convenient, without a great loss in generality, to assume that the spring factors (α_r) and (α_{cr}), the coupling parameters $(\bar{g}_r)$ and $(\bar{m}_{cr})$ and the modal overlap parameters (b_r) and (b_{cr}) are to be independent of (r); namely

$$\alpha_r = \alpha; \quad \alpha_{cr} = \alpha_c; \quad \bar{g}_r = \bar{g}; \quad \bar{m}_{cr} = \bar{m}_c; \quad b_r = b_{cr} = b, \tag{15}$$

and it is observed, as already intimated, that the modal overlap parameters (b_r)

and (b_{cr}) are set equal to (b). [cf. Appendix A.] From Eqs. (9c), (10), (11) and (12), one then finds

$$(\alpha + \alpha_c) = (1 + \bar{m}_c)\,, \tag{9d}$$

$$\eta_r = \eta_{cr} = \eta_{rr} = \eta(\bar{r}); \quad \eta(\bar{r}) = (\bar{b}/\pi)\,[\gamma(\bar{R})(x_r^o)^2\,], \tag{16}$$

where

$$\bar{b} = [(\pi b)\,(R+1)^{-1}\,]. \tag{17}$$

Under this imposition, the two-vector $\{(x_{rr}), (\eta_{rr})\}\,(R)$ assumes the simple form

$$\{(x_{rr}), (\eta_{rr})\}\,(R) = \{(1+\bar{m}_c)^{1/2}(x_r^o), \eta(\bar{r})\}, \tag{18a}$$

and, if further, the mass coupling parameter $(\bar{m}_c)$ is negligible; $(\bar{m}_c) << 1$, then

$$\{(x_{rr}^o), (\eta_{rr}^o)\}\,(R) = \{(x_r^o), \eta(\bar{r})\}, \tag{18b}$$

where the superscript (o) in (x_{rr}) and (η_{rr}) recognizes that (x_{rr}^o) and (η_{rr}^o) are restricted to specific impositions. [cf. Eq. (4).] With $R = 27$ and $\bar{m}_c = 0$, Eq. (18) is evaluated and depicted in Fig. 2a, as a function of $(\bar{r})$; Fig. 2a.1 depicts (x_{rr}) and Fig. 2a.2 depicts (η_{rr}). In Fig. 2a the modal overlap parameter (b) is increased from (0.1) to (2.0) and then onto (10). To these changes (η_{rr}) increases by a factor of (20) and then by a factor of (10^2), whereas, to these changes in (b), (x_{rr}) remains intact. With R = 7 and $\bar{m}_c = 0$, Eq. (18) is evaluated and depicted, in the format of Fig. 2a, in Fig. 2b. On the other hand, with R = 27, but with $\bar{m}_c = 0.75$, where, for example, in addition $\alpha = 1.75$, $\alpha_c = \bar{g}_c = 0$, Eq.

(18) is evaluated and depicted, in the format of Fig. 2a, in Fig. 2c. It is noted that for a continuous r, except for obvious end conditions, Figs. 2a.1 and 2b.1 are identical. However, Figs. 2a.2 and 2b.2 are not identical. On the other hand, it is noted that Figs. 2a.2 and 2c.2 are identical, however, Figs. 2a.1 and 2c.1 are not identical. The commonalties and disparities among Figs. 2a, 2b and 2c, are as expected. [It is also noted, in passing, that (x_{rr}) and (η_{rr}), stated in Eq. (18) are independent of the gyroscopic coupling parameter $(\bar{g}_r)$.]

It remains then to use the two-vector stated in Eq. (18) to evaluate the induced loss factor $\eta_s(y)$. Indeed, using Eq. (18) in Eq. (8b), one derives the more explicit expression for $\eta_s(y)$ in the form

$$\eta_s(y) = -(y)^2 \,\mathrm{Im}\left\{\sum_1^R \bar{m}_r \{[1-\alpha(z_r^o)^2\{1+i\eta(\bar{r})\}]\,[\bar{m}_c - \alpha_c(z_r^o)^2\{1+i\eta(\bar{r})\}]\right.$$

$$-4\bar{m}_c\,\alpha_c\,(z_r^o)^2\{1+i\eta(\bar{r})\}-(\bar{g}/y)^2\}\cdot$$

$$\left.[(1+\bar{m}_c)-(\alpha+\alpha_c)(z_r^o)^2\{1+i\eta(\bar{r})\}]^{-1}\right\};\quad z_r^o = (x_r^o/y), \qquad (8d)$$

where $(\bar{m}_c)$, $(\bar{g})$, (y), (α), (α_c), (x_r^o), $(\bar{m}_r)$ and $\eta(\bar{r})$ are stated in Eqs. (1d), (3a), (11), (12), (14) and (16), respectively. The computations of $\eta_s(y)$ are largely carried out assigning the standard values

$$(M_s/M) = 10^{-1},\ b = (0.1) \text{ and } \mathrm{R} = 27, \qquad (19)$$

where (M_s) is stated in Eq. (14), (b) is the modal overlap parameter and (R) is the number of satellite oscillators in the set. When these standard assignments are deviated from, specific mentions are to be rendered, notwithstanding that, at times, the employment of these standard values may be reiterated.

III. Revisiting the Results Presented in Reference 1

It may be useful, at this stage, to reproduce results that are depicted in Reference 1. To this end, the following impositions are rendered

$$\alpha \Rightarrow 0\,; \quad \alpha_c = 1; \quad \bar{m}_{cr} = 0; \quad \bar{g}_r = 0. \tag{20}$$

These impositions render the complex commensurate with that defined in Reference 1 and sketched in Fig. 1a. [cf. Fig. 1b.] For these impositions, Eqs. (16) and (18b) and Fig. 2a are validated. One finds that Figs. 2a.1 and 2a.2 are akin to Figs. 3a and 7a of Reference 1, respectively. In addition to evaluating the two-vector specified in Eqs. (16) and (18b), the corresponding induced loss factor $\eta_s^o(y)$ is evaluated using Eq. (8d) and the assignment stated in Eqs. (19) and (20). Again, the superscript (o) in $\eta_s(y)$ indicates that the evaluation is restricted to specific impositions. This evaluation of $\eta_s^o(y)$ is depicted in Fig. 3a. The modal overlap parameter (b) is increased from the value of (0.1) to (2.0) and then onto (10) and $\eta_s^o(y)$ is evaluated and depicted in Figs. 3b and 3c, respectively. The identity of Figs. 3a and 3b with Figs. 5a and 6a of Reference 1, respectively, is clear. In particular, the undulations that exist in Fig. 3a and the suppression of these undulations in Fig. 3b corresponds to a phenomenon that is discussed in detail in Reference 1. Figure 3c does not have a counter part in Reference 1. This figure is included in order to bring in another phenomenon;

the phenomenon of erosion that may beset the induced loss factor $\eta_s(y)$ [1-3]. It transpires that mean-value averaging of levels of $\eta_s(y)$, for modal overlap parameters (b) that are small compared with unity, coincide and are thus independent of (b) [1, 14]. This coincidence is illustrated in Fig. 3d. In this figure $\eta_s(y)$ is depicted for three small values of the modal overlap parameter (b); $b = (0.01), (0.1)$ and (0.3). The coincident curve representing the mean-values of $\eta_s(y)$ for all small values of (b); $b << (1.0)$, clearly emerges in Fig. 3d. For reasons that are explained subsequently, the curve coincident with these mean-values is dubbed (FOA). An erosion is here a phrase to describe deviations of the levels of $\eta_s(y)$ from these mean-values when (b) approaches and increases beyond the value of unity. An erosion is then a dependence of the levels of $\eta_s(y)$ on (b) as this parameter approaches and exceeds unity. To bring into focus the existence and nature of erosion for $\eta_s(y)$, Figs. 3a, 3b and 3c are overlaid in Fig. 3e. Also, superimposed on Fig. 3e is the curve just designated (FOA). The presence of erosion, as just described, is thus revealed in Fig. 3e. It is apparent that erosions commence at the edges of the normalized frequency range; the higher the value of the modal overlap parameter (b) above unity, the more the inroad from the edges into the frequency range. (The frequency range of reference is that spanning the resonance frequency distribution of the satellite oscillators.) Figure 3e, however, shows that there is hardly any erosion at and in

the vicinity of y=1. One is reminded that this is precisely the normalized frequency region where $\eta_s(y)$ potentially plays the more significant role in controlling the response behavior of the master oscillator. To cause an erosion at and in the vicinity of y=1, the normalized overlap parameter $(\bar{b})$; $\bar{b} = [(\pi b)(R+1)^{-1}]$, needs approach and exceeds unity [1-3]. This extreme case of erosion is illustrated in Fig. 3f. In this figure the only change, in parameters that specify the complex assigned to Fig. 3e, is the number (R) of satellite oscillators. The number (R) is (7) instead of (27), so that for b = 10, $(\bar{b})$ comfortably exceeds unity in Fig. 3f. After this brief digression, it is time to return to consideration of Reference 1 and beyond.

The limited scope of Reference 1 curtails the modeling and the analysis of the complex there considered, notwithstanding that complexes employed to date are largely subjected to similar limitations [2-11]. A poignant question arises: what is fresh about the complex defined herein as compared with the complex defined in Reference 1? Whereas in Reference 1 a satellite oscillator in isolation is characterized by a mere mass control term, here it is characterized by the oscillator impedance $Z_r(\omega)$, as stated in Eq. (3b). This oscillator, in addition to the mass control term, may also possess a stiffness control term. Moreover, the coupling impedance $Z_{cr}(\omega)$, as stated in Eq. (3c), may, in addition to the stiffness control term, possess also a mass control term. Finally, the coupling between a satellite oscillator and a master oscillator may be allowed to include a

gyroscopic control term [12, 13]. Obviously, the complex sketched in Fig. 1b and formulated in Eqs. (5) – (8) is more versatile than that in Reference 1, as sketched in Fig. 1a. It may be useful, therefore, to investigate a few of the attributes of this versatility even under the similarity conditions imposed in Eq. (11) and the simplifying assumptions proposed in Eqs. (14) and (15).

IV. Various Coupling Forms and Coupling Strengths

It is of interest to evaluate the induced loss factor $\eta_s(y)$, as a function (y), for a variety of selected coupling forms and coupling strengths. The coupling forms are defined according to whether the coupling is dominated by either a stiffness coupling, a gyroscopic coupling, a mass coupling or combinations of these coupling types. The coupling strengths of these forms are determined by the values of the coupling parameters; the stiffness coupling parameter (α_c), the gyroscopic coupling parameter $(\bar{g})$; $\bar{g}_r = \bar{g}$, and the mass coupling parameter $(\bar{m}_c)$. The values of these coupling parameters may be categorized from weaker-coupling, to moderate-coupling onto stronger-coupling in the range of values of 0.03, 0.15 and 0.75, respectively. In this categorization, the coupling of the satellite oscillators to the master oscillator, defined in Reference 1, is of stiffness control coupling form; i.e., $\alpha_c \neq 0$, $\bar{g} = \bar{m}_c = 0$, and of (very) strong coupling strength; namely, $\alpha_c = 1.0$ [α=0.0.]. Such a coupling form and a coupling strength define satellite oscillators commonly designated sprung-masses [1-11]. The new evaluations in this paper are exhibited in Figs. 4-7. Of significance are not only the variations in the coupling forms and in the coupling strengths, but, also, the influence that changes in the modal overlap parameters have on the nature of the induced loss factor $\eta_s(y)$. A first set of figures is evaluated with $b = (0.1)$, a second with b=(2.0) and a third with b=(10). A major feature, common to all evaluations, is that the undulations in the first set, for which b=(0.1), is suppressed in the second and in the third, for which

$b=(2.0)$ and $b=(10)$, respectively [1]. Figures 4-7 are cast in the format of Fig. 3e; corresponding figures in the three sets are overlaid so that the undulations in the first set and their suppression in the second and third are observed at a glance. Another major feature, common to all evaluations, is that the erosions, discussed briefly in Section III with respect to $\eta_s(y)$ and depicted in Figs. 3e and 3f, thread all figures. It is noted that when $\bar{b} = [(\pi b)(R+1)^{-1}]$ approaches and exceeds unity, erosions occur even at and in the vicinity of $y=1$. These extreme erosions, however, in addition to the dependence on $(\bar{b})$, seem to carry a slight dependence on the coupling forms and strengths. These dependencies, which are more clearly apparent when the coupling is weak; e.g., in Figs. 6b and 7d, are, at this stage, merely noted. Supplementally, some of the emerging details in Figs. 4-7 may be summarized as follows:

1. The format of Fig. 3e is reproduced in Fig. 4a, except that the stiffness coupling parameter is reduced from $\alpha_c = 1.0$ to $\alpha_c = 0.75$; i.e., from very strong to strong stiffness control coupling . This change decreases the levels in Fig. 4a as compared with those in Fig. 3e. The decrease is, however, slight. A more drastic decrease in levels occurs in Fig. 4b as compared with Fig. 3e. In Fig. 4b the stiffness coupling parameter is $\alpha_c = 0.15$, whereas in Fig. 3e $\alpha_c = 1.0$. This decrease in levels is largely related to the difference in the coupling strengths. In Fig. 4b the coupling strength is moderate.

2. The format of Figs. 4a and 4b is reproduced in Figs. 5a and 5b, respectively, except that the stiffness coupling form is changed to a gyroscopic coupling form; namely, $\alpha_c = \bar{m}_c = 0$, $\bar{g} \neq 0$. In Fig. 5a the coupling is strong; $\bar{g} = 0.75$, and in Fig. 5b the coupling is moderate; $\bar{g} = 0.15$. The similarity between Figs. 4 and 5 is obvious. Also obvious is the slope in the curves in Fig. 5. This slope is characteristic of the gyroscopic coupling. The gyroscopic coupling enters in the form of $(\bar{g}/y)$ and not merely in the form of $(\bar{g})$. [cf. Eq. (8).]

3. The format of Figs. 4a and 4b is reproduced in Figs. 6a and 6b, respectively, except that the stiffness coupling form is changed to a mass coupling form; namely, $\alpha_c = \bar{g} = 0$, $\bar{m}_c \neq 0$. In Fig. 6a the coupling is moderate; $\bar{m}_c = 0.15$, and in Fig. 6b the coupling is weak; $\bar{m}_c = 0.03$. The similarity between Figs. 4 and 6 is obvious although the levels in the former are higher than in the latter, largely in consequence of the disparities in the coupling strengths.

4. Finally, the format of Fig. 4a is reproduced in Fig. 7, except that the stiffness coupling form is modified to accommodate, in addition, another form of coupling. In Fig. 7a the additional coupling form is mass control; namely: $\alpha_c = \bar{m}_c = 0.75[\alpha = 0.1.]$, $\bar{g} = 0$, which is a very strong coupling strength. In Figs. 7b, 7c and 7d, the additional coupling is gyroscopic control; namely, in Fig. 7b: $\alpha_c = 0.53$ $[\alpha = 0.43.]$, $\bar{g} = 0.54$, $\bar{m}_c = 0$, which is a strong coupling strength, in Fig. 7c: $\alpha_c = 0.10$ $[\alpha = 0.9.]$, $\bar{g} = 0.11$, $\bar{m}_c = 0$, which is a moderate coupling strength and finally, in Fig. 7d: $\alpha_c = 0.02[\alpha = 0.98.]$, $\bar{g} = 0.022$, $\bar{m}_c = 0$, which

is commensurate with a weak coupling strength. The levels in these figures are set largely by the coupling strengths; the higher the coupling strength the higher the levels.

In the normalized frequency range of concern, the levels in Figs. 3-7 that pertain to modal overlap parameters (b) that are small compared with unity; e.g., $b = (0.1)$, undulate. On the other hand, again in the normalized frequency range of concern, the curves in Figs. 3-7 that pertain to modal overlap parameters that exceed unity; e.g., b=(2.0) and (10), are reasonably smooth. A few questions arise: Can these features be estimated by replacing the summation in Eq. (8d) by an integration and if so, can this integral be performed with ease? Can the result of this performance interpret the response behavior of the master oscillator in terms of the various parameters that define the complex? And last, but by no means least, what about the undulations, do they feature in the result of this integration?

V. Replacing a Summation by an Integration

The index (r) is given a continuous connotation and the summation in Eq. (8b) is replaced by integration. Under a condition that allows this replacement, Eq. (8b) assumes the form [1]

$$[S(y) - i\eta_s(y)] = (y)^3 \int_{z_r(\bar{\varepsilon})}^{z_r(\bar{R}+\bar{\varepsilon})} dz_r(\bar{r})\,[f(r)\mu(\bar{r})]\,\bullet$$

$$\{[1 - \{z(\bar{r})\}^2 (1+i\eta(\bar{r}))]\,[\bar{m}_c(r) - \{z_c(\bar{r})\}^2 (1 + i\eta_c(\bar{r}))] - [\bar{q}_c(\bar{r})/y]^2\}\,\bullet$$

$$\{[1+\bar{m}_c(\bar{r})] - [\{z_r(\bar{r})\}^2 (1+i\eta_r(\bar{r}))]\}^{-1} \qquad (21)$$

where

$$[\bar{q}_c(\bar{r})/y]^2 = 4\bar{m}_c(\bar{r})\,\{z_c(\bar{r})\}^2 (1+i\eta_c(\bar{r})) + [(\bar{g}(\bar{r})/y]^2;$$

$$\bar{m}(\bar{r}) = \mu(\bar{r})(R+1)^{-1};\; f(\bar{r})dz_r(\bar{r}) = d\bar{r};\; \{z_r(\bar{r})\}^2 = \{z(\bar{r})\}^2 + \{z_c(\bar{r})\}^2;$$

$$\bar{\varepsilon} = \varepsilon(R+1)^{-1};\; (\bar{R}+\bar{\varepsilon}) = (R+\varepsilon)(R+1)^{-1} \qquad (22)$$

If $\eta_r(\bar{r})$ is small enough so that the vanishing of the real part of the denominator in the integral in Eq. (20) predominates the values of the integral, the integral yields

$$\{S(y)-i\eta(y)\}=(\pi/2)y^3[f(\bar{r}_o)\mu(\bar{r}_o)][1+\bar{m}_c(\bar{r}_o)]^{-(1/2)}[\{[\bar{m}_c(\bar{r}_o)-\{z_c(\bar{r}_o)\}^2]\cdot$$

$$[\{z(\bar{r}_o)\}^2\eta(\bar{r}_o)-\{z_c(\bar{r}_o)\}^2\eta_c(\bar{r}_o)]+4\bar{m}_c(\bar{r})\{z_c(\bar{r}_o)\}^2\eta_c(\bar{r}_o)\}$$

$$-i[\bar{m}_c(\bar{r}_o)-\{z_c(\bar{r}_o)\}^2]^2+[\{z(\bar{r}_o)z_c(\bar{r}_o)\}^2\eta(\bar{r}_o)\eta_c(\bar{r}_o)]+[\bar{q}_c(\bar{r}_o)/y]^2\}], \qquad (23)$$

where

$$(\bar{\varepsilon})<\bar{r}_o<(\bar{R}+\bar{\varepsilon});$$

$$\{z_{r_o}(\bar{r}_o)\}^2=(1+\bar{m}_{cr})=\{z(\bar{r}_o)\}^2+\{z_c(\bar{r}_o)\}^2;$$

$$\{z_{r_o}(\bar{r}_o)\}^2\,\eta_{r_o}(\bar{r}_o)=\{z(\bar{r}_o)\}^2\eta(\bar{r}_o)+\{z_c(\bar{r}_o)\}^2\eta_c(\bar{r}_o). \qquad (24)$$

Equation (24) defines the specific value of $(\bar{r}_o)$ and it is recognized that $(\bar{r}_o)$ is a function of (y) and vice versa. Adopting the impositions and the simplifications that are conducted in Eqs. (16) and (18), one may derive from Eqs. (23) and (24) the result

$$\eta_s(y)=D[C+O\{\eta(y)\}^2];\quad \eta_s(y)\Rightarrow\eta_I(y)=DC, \qquad (25)$$

with

$$D=[\pi/2\gamma(\bar{R})][M_s/(M\bar{R})][(1+\bar{m}_c)]^{-1}, \qquad (26a)$$

$$C=[(\bar{m}_c+\alpha_c)^2+(\bar{g}/y)^2], \qquad (26b)$$

$$O=[(1+\bar{m}_c-\alpha_c)\alpha_c], \qquad (26c)$$

and where

$$f(\bar{r}_o)=[(\alpha+\alpha_c)^{(1/2)}\gamma(\bar{R})(y)^3\,]^{-1};\quad \mu(\bar{r}_o)=(M_s/M\bar{R}), \tag{26d}$$

$$\eta(y)=\eta(\bar{r}_o)=(\bar{b}/\pi)[\gamma(\bar{R})(y)^2\,];\quad \eta(\bar{r}_o)=\eta_c(\bar{r}_o)=\eta_{r_o}(\bar{r}_o), \tag{26e}$$

$$(1+\bar{m}_c)=(\alpha+\alpha_c);\qquad [1+(\gamma/2)]^{-(1/2)}\le y\le [1-(\gamma/2)]^{-(1/2)}\,. \tag{26f}$$

The underlying condition of the validity on Eq. (25) is detailed in Reference 1. This condition holds even though the coupling forms are elaborated to include not only a weaker stiffness coupling, but also mass and gyroscopic coupling forms. Moreover, the coupling parameters may define various degrees of coupling strengths. Strictly, the validity of Eq. (25) demands the equality of $\eta_s(y)$ to the *primary term* $\eta_I(y)$. This equality designates $\eta_I(y)$ the first order approximation to $\eta_s(y)$. The term $O\{\eta(y)\}^2$ is of the order of the higher approximations to the integral, notwithstanding that situations exist in which (O) is identically zero; e.g., when the satellite oscillators are sprung-masses for which $\alpha_c=1,\quad \bar{g}=\bar{m}_c=0$. [cf. Eq. (20).] In these situations the equality of the integral evaluation of $\eta_s(y)$ to $\eta_I(y)$ need not be specifically invoked. (More on this subject when in a subsequent paper higher order of approximations, than the first, are to be evaluated.) Clearly and significantly, the primary term $\eta_I(y)$ and, therefore, the first order approximation of $\eta_s(y)$ is independent of the modal overlap parameter (b). Without much-a-do, in this paper the first order approx-

imation only is implemented and considered. In this approximation the *first order approximation* to $\eta_s(y)$ is the primary term $\eta_I(y)$.

Equation (25) reveals the parametric composition of the first order approximation to the induced loss factor $\eta_s(y) \Rightarrow \eta_I(y)$. Again, one is reminded that the induced loss factor $\eta_s(y)$ describes the influence of the coupled satellite oscillators on the loss factor in the impedance of the master oscillator. In the absence of couplings this loss factor is (η_o); in the presence of couplings it is $[\eta_o + \eta_s(y)]$. Since the satellite oscillators add merely passive elements to the complex, $\eta_s(y)$ is invariably positive. Equation (25) confirms this statement and exposes the proportionality of $\eta_I(y)$ to (D). Therefore, $\eta_I(y)$ is directly proportional to the mass ratio (M_s / M); it is estimated that for a reasonable complex with (M_s / M) equal to about a tenth, (D) is of the order of unity. [cf. Eq. (19).] The quadratic dependence of the primary term $\eta_I(y)$ of $\eta_s(y)$, in terms of (C), which entertain the term-components $(\bar{m}_c + \alpha_c)^2$ and $(\bar{g}/y)^2$, is of significance. Again, it is emphasized that the primary term $\eta_I(y)$ is the *true* first order approximation to $\eta_s(y)$; in this context the term $DO\{\eta(y)\}^2$ is superfluous. In any case, Eq. (26) indicates that this term in $\eta_s(y)$ is rarely dominant even when the loss factor $\eta(y)$ of a typical satellite oscillator exceeds any of the coupling parameters; $\bar{m}_c, \alpha_c, (\bar{g}/y) \leq \eta(y)$, notwithstanding that in the absence of any couplings $\eta_s(y)$, as stated in Eq. (25), is negligible on account of both, $C = 0$ and $O = 0$. On the other hand when couplings do exist, in both, the first order approximation and the exact evaluations of $\eta_s(y)$, the levels are certainly not

negligible, even if the couplings are weak. [Note that (η_o) of the order of (10^{-4}) is not unreasonable [12].]

As already discussed and demonstrated in Figs. 3-7 the curves for a modal overlap parameter (b) that is small compared with unity; $b << 1$, possess levels that are undulated. The excursions in the undulations are the more pronounced the smaller is the value of (b) [11]. [cf. Fig. 3d.] As (b) increases, approaching and exceeding unity, the undulations, again true to form, are suppressed. As already intimated in Section III, increasing (b) beyond unity brings in the phenomenon of erosion which worsens as the modal overlap parameter (b) reaches higher and higher above unity. A remarkable property of the first order approximation (FOA) of $\eta_s(y)$ $[\equiv \eta_I(y)]$ emerges when this quantity is superimposed on the respective Figs. 4-7. [cf. Figs. 3d, 3e and 3f.] It is now observed, in these figures, that the mean-value averaging of the undulations of the exact levels of $\eta_s(y)$, when (b) is small compared with unity; $b << 1$, converges onto the first order approximation (FOA) of $\eta_s(y)$ [1, 14]. Since, as already observed, the first order approximation; namely, $\eta_I(y)$, is independent of (b) this convergence is without erosion and, of course, remains so. [cf. Figs. 3d and 3e.] The independence of $\eta_I(y)$ of (b) has been stretched by some to conclude that (b) may be rendered, a priori, equal to zero. Neglecting to mention in this rendering that mean-value averaged levels are substituted for highly undulated levels, is not a viable scientific procedure, unless ignorance is bliss [11]. On the other hand, when (b) approaches and exceeds unity, the exact levels become free of undulations, but these levels erode with further increases of

(b). The erosion in the exact levels, when (b) increases beyond unity, commences and progresses from the levels of the first order approximations. To account for this progressive dependence on (b), higher order approximations are clearly required. What is doubtful is whether higher and higher order approximations can account for the undulations when (b) needs to remain small compared with unity. To account for the undulations an entirely different approximation procedure is thus called for. In this paper devising such an approximation procedure is not attempted.

VI. A Typical Member of an Ensemble of Complexes Supporting Various Parametric Combinations

In the preceding evaluations the distribution of resonance frequencies (x_{rr}) and the assigned loss factors (η_{rr}) for the satellite oscillators are sequential functions of the normalized index $(\bar{r})$. These two quantities, exemplified in Figs. 2a.1, 2b.1 and 2c.1 and in Figs. 2a.2, 2b.2 and 2c.2, respectively, may be smoothed out by extrapolation and interpolation into monotonic and continuous functions of $(\bar{r})$; $(\bar{r})=[r(R+1)^{-1}]$. This kind of smoothness is rarely found in practice and a question arises as to what are the expected consequences of more practical assignments for these parameters and others? In this section a few layers are removed in the quest to discover the phenomena that may be encountered in the induced loss factor $\eta_s(y)$ by the insertion of these more realistic parametric values. Since the assignment for the parameters that define the satellite oscillators and their couplings to the master oscillator can hardly be drawn, a more generalized approach is undertaken to investigate the influence of introducing variations in these parametric values. In particular, in this section two parameters are selected to carry these variations; either individually or in unison. In the first, the index (r) of a satellite oscillator is assigned a pseudo-statistical value. [Pseudo-statistical is in reference to a sample selected out of an

ensemble of random samples.] The index (r) is distributed sequentially and fractionally, in the range $1 \leq r \leq 27$. A pseudo-statistical index is designated $\Lambda(r)$, where $\Lambda(r) \leq \Lambda(q)$; $q = (r+1)$; $1 \leq r \leq (R-1)$. [cf. Eq. (9b).] In the second, the modal overlap parameter (b_r) is assigned a pseudo-statistical value that is distributed in the ranges $(2) \geq b_r \geq (0.1)$ and $(3.5) \geq b_r \geq (1)$, respectively. The distribution of $\Lambda(r)$ and of (b_r), with $R = 27$, that are employed in this section are depicted graphically in Figs. 8a, 8b, and 8c. The two-vector $\{(x_{rr}), (\eta_{rr})\}(R)$, as stated in Eqs. (16) and (18), is typically depicted, for the pseudo-statistical values shown in Figs. 8a, 8b, and 8c, in Figs. 9a, 9b, and 9c, respectively. Figure 9a depicts (x_{rr}) as a function of $\bar{\Lambda}(r)$ and Figs. 9b and 9c depict (η_{rr}), as a function of $(\bar{r})$, where $\bar{\Lambda}(r) = [\Lambda(r)(R+1)^{-1}]$ and $\bar{r} = [r(R+1)^{-1}]$. [cf. Fig. 2a.] It is observed, in Fig. 9a, that the pseudo-statistical variations embody the phenomenon of mode bunching in which variations in the modal density of the satellite oscillators drastically vary as a function of $\Lambda(r)$ [17]. On the other hand, as Figs. 9b and 9c show, the loss factor (η_{rr}), as a function of (r), faithfully follows the variations assigned to (b_r). In Fig. 9b some of the values of (b_r) are less than unity, in Fig. 9c all the values of (b_r) are in excess of unity.

The influence of the variations, described in Fig. 8, on the induced loss factor $\eta_s(y)$, as a function of (y), is exemplified in Figs. 10 and 11. Each figure

represents a set of figures. The first figure in each set; e.g., Fig. 10a, depicts the base situation in which $\bar{\Lambda}(r) = \bar{r}$ and $b_r = 1$. The second figure in each set; e.g., Fig. 10b, depicts the situation in which $\bar{\Lambda}(r)$ is as shown in Fig. 8a and $b_r = 1$. The third figure in each set; e.g., Fig. 10c, depicts the situation in which $\bar{\Lambda}(r) = r$ and (b_r) is as shown in Fig. 8b. The fourth figure in each set; e.g., Figure 10d, depicts the situation in which $\bar{\Lambda}(r) = r$ and (b_r) is as shown in Fig. 8c. The fifth figure in each set; e.g., Fig. 10e, depicts the combined situation in which $\bar{\Lambda}(r)$ and (b_r) are as shown in Figs. 8a and 8b, respectively. Finally, the sixth figure in each set; e.g., Fig. 10f, depicts the combined situation in which $\bar{\Lambda}(r)$ and (b_r) are as shown in Figs. 8a and 8c, respectively. It is recognized then that each set of figures presents a complete evolution in the process of applying the pseudo-statistical variations depicted in Fig. 8 to the two parameters $\bar{\Lambda}(r)$ and (b_r). Also, each set selects a specific coupling form and a specific coupling strength. Thus, Fig. 10 pertains to a *strong* stiffness coupling: $\alpha_c = 1.0$ [$\alpha = 0.0$.], $\bar{m}_c = \bar{g} = 0$, and Fig. 11 pertains to a mix of stiffness and of gyroscopic coupling of *moderate* strength: $\alpha_c = 0.1$[$\alpha = 0.9$.], $\bar{g} = 0.11$, $\bar{m}_c = 0$. [cf. Figs. 3e and 7c.]

The first figure of each set; namely, Figs. 10a and 11a exhibit undulations in the levels of the induced loss factor $\eta_s(y)$, as a function of (y). However, these undulations are small and they are completely suppressed as soon

as (b_r) approaches the value of (2). [cf. Fig. 3b.] The variations depicted in Fig. 8 are clearly discernible in all the subsequent figures in the series entitled Figs. 10 and 11. True to form, there is but a tinge of edge erosion in Figs. 10a and 11a, yet in the likes of Fig. 3b stronger sign of erosion has already reared its head. From Figs 10a and 11a to Fig. 3b, (b) is changed from unity to merely two. To confirm this statement and to provide for convenient and interpretable data from which to judge the more erratic data that incorporates the pseudo-statistical variations, the first order approximation of $\eta_s(y)$, given in Eq. (25), is superimposed on Figs. 10a and 11a and on all other figures in the series entitled Figs. 10 and 11.

Again, the pseudo-statistical variations are defined by two competing and nearly independent factors, i.e., by $\Lambda(r)$ and $b(r)[=(b_r)]$. In Figs. 9a, 10b and 11b; it is observed that at a mode bunching (a rich modal density) region the influence of the satellite oscillators is more pronounced than at a mode sparsity (a poor modal density) region [17]. On the other hand, when the modal overlap parameter (b_r) entertains values that are small compared with unity, the levels as a function of (y), tend to fluctuate. The fluctuations are pronounced at and in the vicinity of the resonance frequencies of those satellite oscillators to which these small values of (b_r) are assigned. At and in the vicinity of the resonance frequencies of those satellite oscillators to which (b_r) are assigned values that approach and exceed unity, no such fluctuations are present; e.g., see Figs. 10c

and 11c, and Figs. 10d and 11d and contrast them, respectively [18]. When variations in both parameters are combined, both characteristics can be identified in the levels of the induced loss factor $\eta_s(y)$; e.g., see Figs. 10 and 11 and contrast, in particular, Figs. 10e and 11e with Figs. 10f and 11f.

Appendix A

The sweeping assumptions rendered in Eq. (15), which leads to Eqs. (9d) and (16), culminating in Eq. (18), may be introduced more gradually. The purpose for this Appendix is to effect such a gradual introduction. In this manner when some of these assumptions are relieved, reevaluation of the induced loss factor $\eta_s(y)$ may be readily instituted.

From Eqs. (9c) and (12), the design demands that

$$(\alpha_r + \alpha_{cr})\,(x_r^o)^2 = (1+\bar{m}_{cr}) \text{ for } \bar{r}=(1/2), \tag{A1}$$

and if (x_r^o) becomes, by design, unity at $\bar{r}=(1/2)$, the expression reduces to

$$(\alpha_r + \alpha_{cr}) = (1+\bar{m}_{cr}) \text{ for } \bar{r} = (1/2). \tag{A2a}$$

From Eq. (12) it is observed with satisfaction that (x_r^o) is, indeed, unity at $\bar{r} = (1/2)$. On the other hand, from Eqs. (10) and (11) one obtains

$$(x_r)^2\,\eta_r = (b_r/2)\,[\partial\{x_r\,(x_r^o)^2\}/\partial r]; \quad (x_{cr})^2\,\eta_{cr} = (b_{cr}/2)\,[\partial\{\alpha_{cr}(x_r^o)^2\}/\partial r];$$

$$\eta_{rr} = [2(\alpha_r+\alpha_{cr})(x_r^o)^2]^{-1}\,\{b_r[\partial\{\alpha_r(x_r^o)^2\}/\partial r] + b_{cr}[\partial\{\alpha_{cr}(x_r^o)^2\}/\partial r]\}, \tag{A3}$$

where again, (r) is allowed to have a continuous connotation as explained in Reference 1. In particular, if the spring factors (α_r) and (α_{cr}) are independent of (r), Eq. (A3) simplifies to read

$$\eta_r = (\bar{b}_r/\pi)[\gamma(\bar{R})(x_r^o)^2]; \quad \eta_{cr} = (\bar{b}_{cr}/\pi)[\gamma(\bar{R})(x_r^o)^2];$$

$$\eta_{rr} = \beta_r \eta_{cr}; \quad \alpha_r = \alpha; \quad \alpha_{cr} = \alpha_c, \tag{A4}$$

where (x_r^o) is extrapolated and interpolated to become a continuous function of (r)

$$[(\partial \ln(x_r^o/\partial r)] = (R+1)^{-1}[\gamma(\bar{R})(x_r^o)^2], \tag{A5}$$

$$(\beta_r b_{cr}) = (\alpha + \alpha_c)^{-1}[(b_r \alpha)+(b_{cr}\alpha_c)], \tag{A6}$$

$$\bar{b}_r = [(\pi b_r)(R+1)^{-1}]; \quad \bar{b}_{cr} = [(\pi b_{cr})(R+1)^{-1}], \tag{A7}$$

and from Eq. (A2a), by design

$$(\alpha + \alpha_c) = (1+\bar{m}_c). \tag{A2b}$$

From Eqs. (10)–(12) and (A2)–(A7) one may cast the designed two-vector in the form

$$\{(x_{rr}), (\eta_{rr})\}(R) = \{(1+\bar{m}_c)^{1/2}, (\beta_r)\} \bullet \{(x_{rr}^o), (\eta_{rr}^o)\}(R), \tag{A8}$$

$$\{(x_{rr}^o), (\eta_{rr}^o)\}(R) = \{(x_r^o), (\bar{b}_{cr}/\pi)[\gamma(\bar{R})(x_r^o)^2]\}, \tag{A9}$$

where

$$\beta_r = \begin{cases} (1+\bar{m}_c)^{-1}[\alpha(b_r/b_{cr})+\alpha_c] & ; \quad b_r \neq b_{cr}, \quad (A10a) \\ = \beta = \begin{cases} (1+\bar{m}_c)^{-1}[\alpha(b/b_c)+\alpha_c]; & b_r = b, \ b_{cr} = b_c \quad (A10b) \\ 1 & ; \quad b = b_r = b_{cr}, \quad (A10c) \end{cases} \end{cases}$$

the quantities $(\bar{m}_c)$, (x_r^o), $\gamma(\bar{R})$ and $(\bar{b}_{cr})$ are stated in Eqs. (1d), (12), (13) and (A7), respectively, and the superscript (o) in (x_{rr}) and (η_{rr}) recognizes that (x_{rr}^o) and (η_{rr}^o) are restricted to specific impositions. [cf. Eq. (4).] For the sake of computational and interpretive advantage the validity of Eqs. (A4) and (A10c) is universally adopted in this paper. [cf. Eq. (15).] Under this imposition, Eqs. (A8) and (A4) simplify

$$\{(x_{rr}),(\eta_{rr})\}(R) = \{(1+\bar{m}_c)^{1/2}(x_r^o), \eta(\bar{r})\}\,; \quad \bar{b} = [(\pi b)(R+1)^{-1}], \tag{A11}$$

$$\eta(\bar{r}) = \eta_r = \eta_{cr} = \eta_{rr}\,; \quad \eta(\bar{r}) = (\bar{b}/\pi)[\gamma(\bar{R})(x_r^o)^2], \tag{A12}$$

where (x_r^o) is stated in Eq. (12), and (β_r) becomes equal to unity. [cf. Eqs. (18a) and (16).]

References

1. G. Maidanik, "Induced damping by a nearly continuous distribution of nearly undamped oscillators: Linear Analysis" 2001, Journal of Sound and Vibration, **240**, 717-731.

2. M. J. Brennan, "Wideband vibration neutralizer," 1997, Noise Control Engineering Journal, **45**, 201-207.

3. G. Maidanik and K. J. Becker, "Noise control of a master harmonic oscillator coupled to a set of satellite harmonic oscillators," 1998, Journal of the Acoustical Society of America, **104**, 2628-2637; "Characterization of multiple-sprung mass for wideband noise control," 1999, Journal of the Acoustical Society of America, **106**, 3119-3127.

4. G. Maidanik, "Power dissipation in a sprung mass attached to a master structure," 1995, Journal of the Acoustical Society of America, **98**, 3527-3533.

5. A Pierce, V. W. Sparrow and D. A. Russell, "Fundamental structural-acoustic idealizations for structures with fuzzy internals," 1995, Journal of Acoustics and Vibration, **117**, 339-348.

6. M. Strasberg and D. Feit, "Vibration damping of large structures by attached small resonant structures," 1996, Journal of the Acoustical Society of America, **99**, 335-344.

7. R. L. Weaver, "Mean and mean-square responses of a prototypical master/fuzzy structure," 1996, Journal of the Acoustical Society of America, **99**, 2528-2529.

8. R. J. Nagem, I. Veljkovic and G. Sandri, "Vibration damping by a continuous distribution of undamped oscillators," 1997, Journal of Sound and Vibration, **207**, 429-434.

9. T. L. Smith, K. Rao and I. Dyer, "Attenuation of plate flexural waves by a layer of dynamic absorbers," 1986, Noise Control Engineering Journal, **26**, 56-60.

10. G. Maidanik and J. Dickey, "Singly and regularly ribbed panels," 1988, Journal of Sound and Vibration, **123**, 309-314.

11. Yu. A. Kobelev, "Absorption of sound waves in a thin layer," 1987, Soviet Physics Acoustics, **33**, 295-296.

12. R. H. Lyon, Statistical Energy Analysis of Dynamical Systems: Theory and Applications, 1975, MIT, Cambridge; and R. H. Lyon and R. G. Dejung, Theory and Application of Statistical Energy Analysis, 1995, Butterworth-Heinemann, Boston.

13. R. H. Lyon and G. Maidanik, "Power flow between linearly coupled oscillators," 1962, Journal of the Acoustical Society of America, **34**, 623-639.

14. E. Skudrzyk, "The mean-value method of predicting the dynamic response of complex vibrators," 1980, Journal of the Acoustical Society of America, **67**, 1105-1135.

15. S. H. Crandall and R. Lotz, "On the coupling loss factor in statistical energy analysis," 1971, Journal of the Acoustical Society of America, **49**, 352-356.

16. G. Maidanik, "Response of coupled dynamic systems," 1976, Journal of Sound and Vibration, **46**, 561-583.

17. G. Maidanik and K. J. Becker, "Modal densities of simple dynamic systems," 1997, Journal of the Acoustical Society of America, **102**, 3130A.

18. M. Strasberg, "When is a "fuzzy" not a fuzzy (Continued)?" 2000, Journal of the Acoustical Society of America, **107**, 2885A.

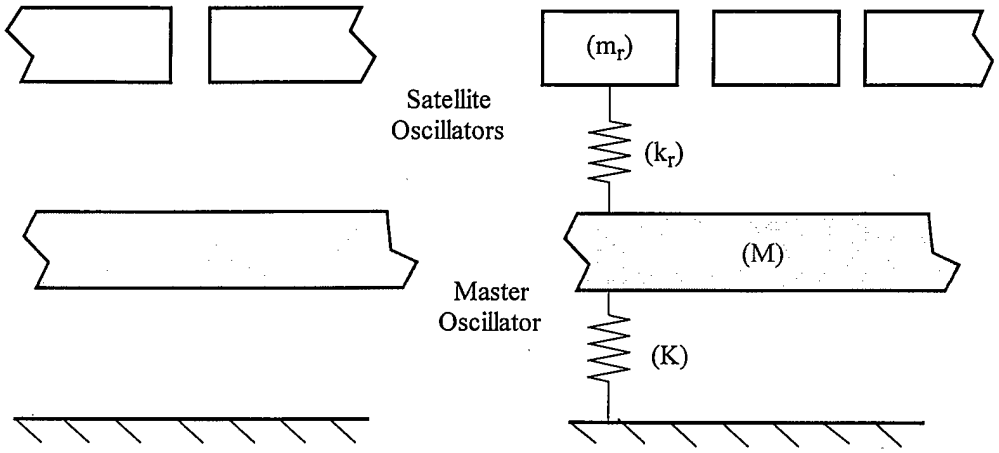

Fig. 1a. A master oscillator attached to a set of sprung-masses.

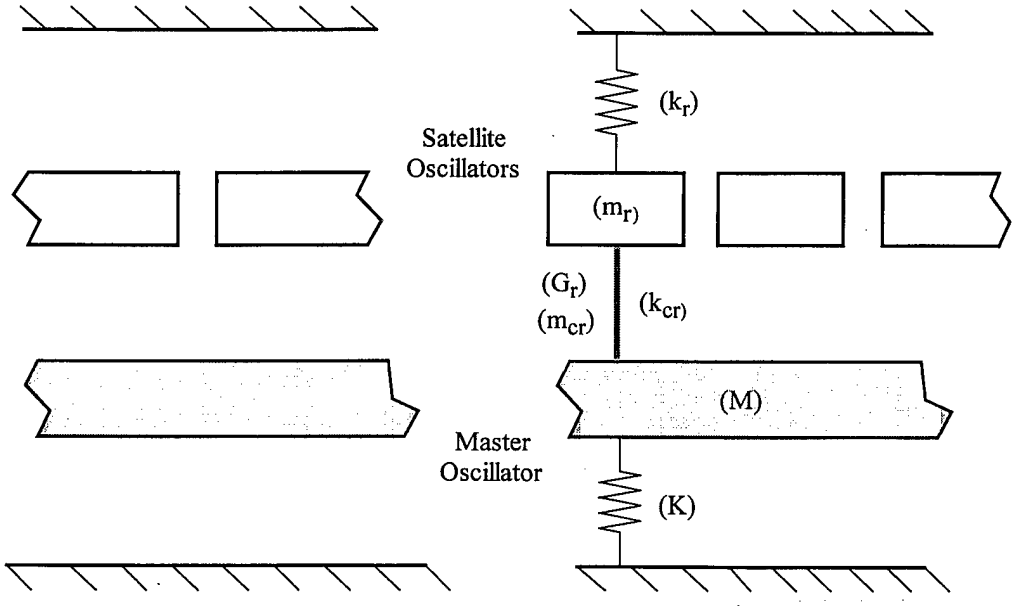

Fig. 1b. A set of satellite oscillators coupled to a master oscillator.

a.1.

a.2.

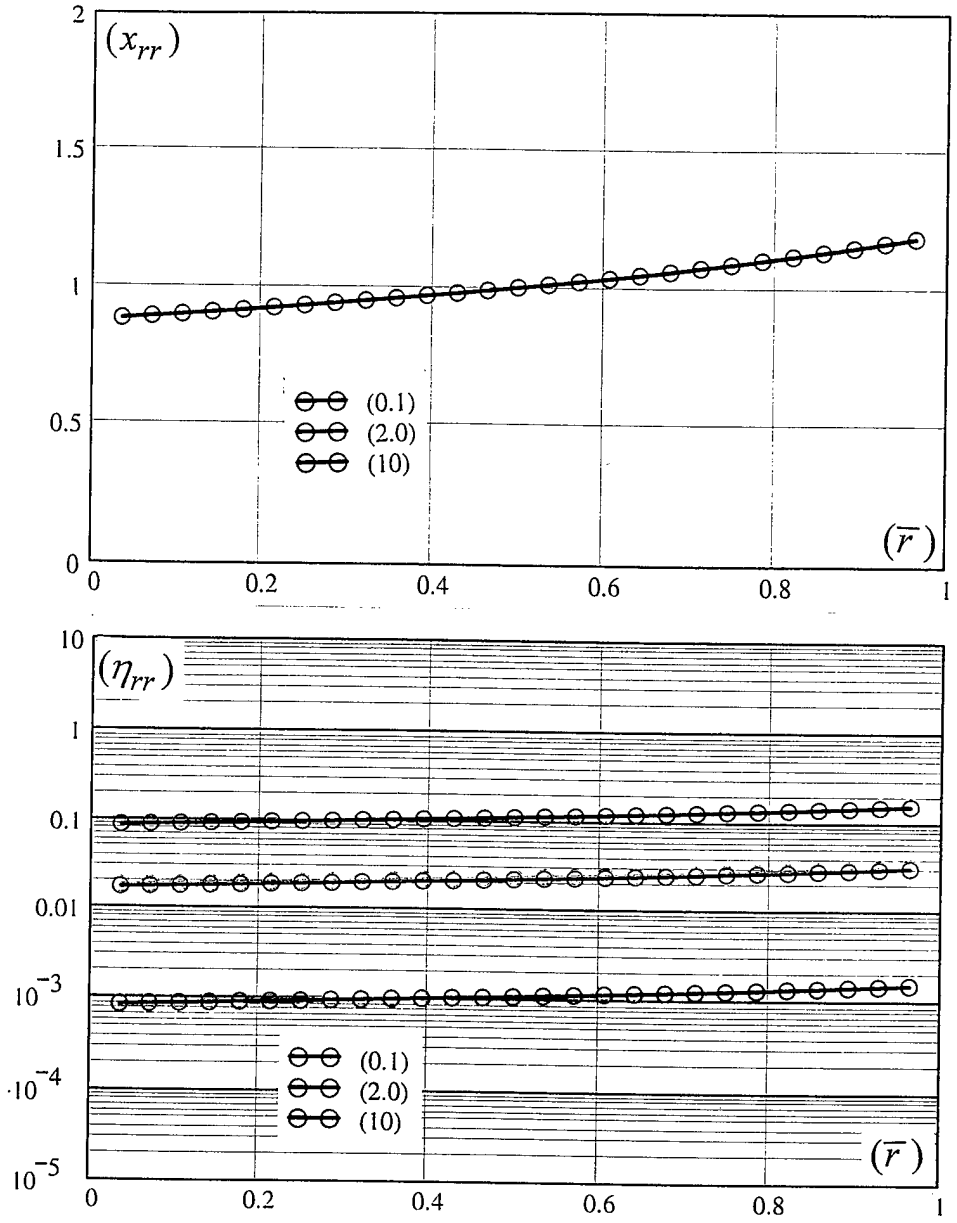

Fig. 2. (1.) Resonance frequency distribution (x_{rr}) and (2.) Corresponding assigned loss factor (η_{rr}) for the satellite oscillators as a function of the normalized index $(\overline{r})$, respectively. (*)

a.1 and a.2. With R = 27 and $\overline{m}_c = 0$. $[x_{rr} = x^o_{rr}\,,\ \eta_{rr} = \eta^o_{rr}\,.]$

(*) When regions of curves clearly overlap, the color of the one with the higher overlap parameter (b) wins.

b.1.

b.2.

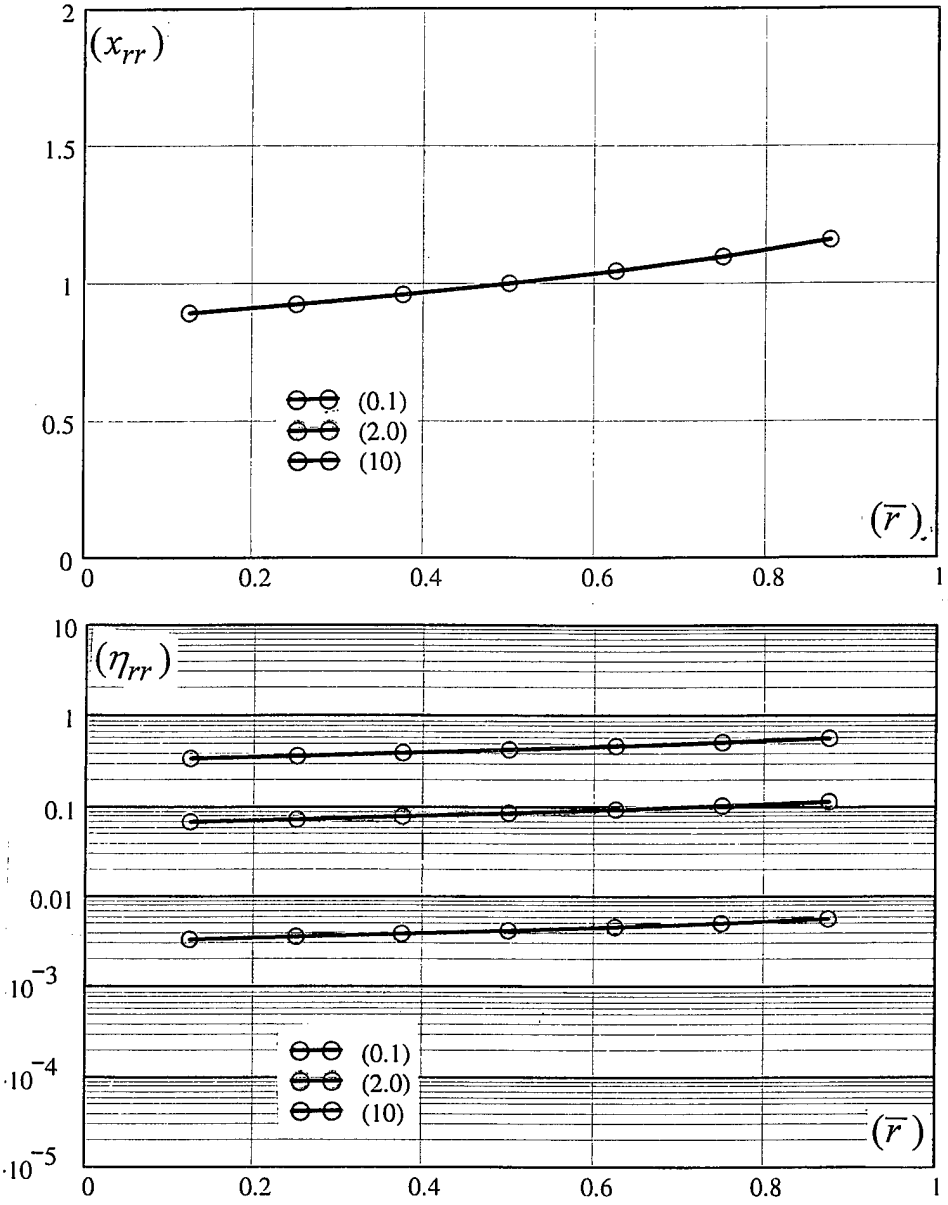

Fig. 2. (1.) Resonance frequency distribution (x_{rr}) and (2.) Corresponding assigned loss factor (η_{rr}) for the satellite oscillators as a function of the normalized index $(\overline{r})$, respectively. (*)

b.1 and b.2. As in a.1 and a.2, except that (R) is changed from (27) to (7).

$[x_{rr} = x_{rr}^{o}, \eta_{rr} = \eta_{rr}^{o}.]$

c.1.

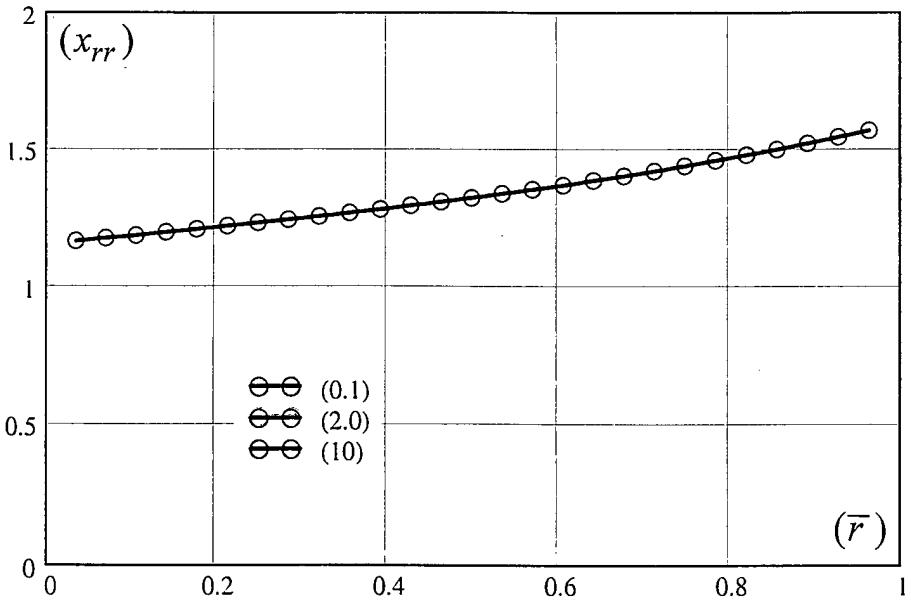

c.2.

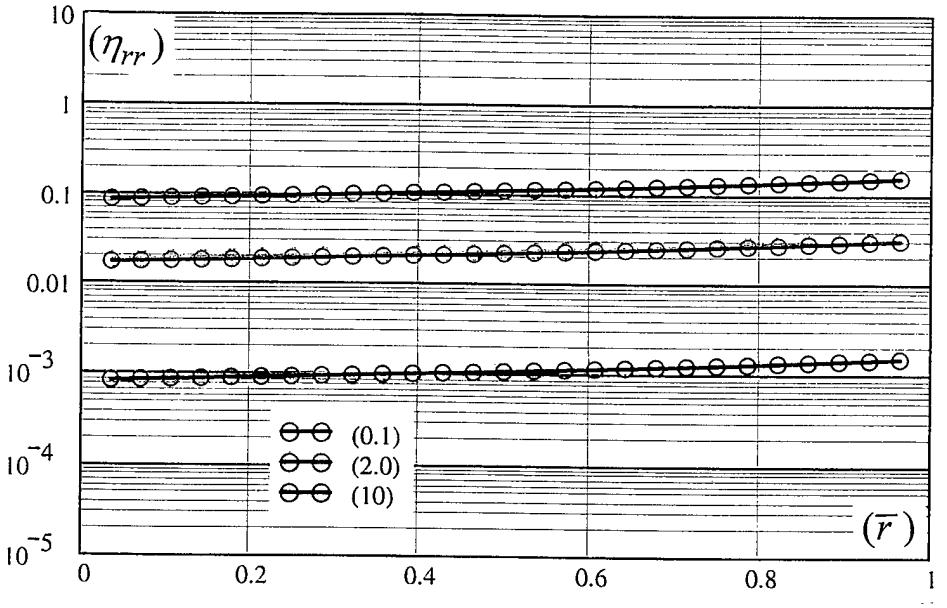

Fig. 2. (1.) Resonance frequency distribution (x_{rr}) and (2.) Corresponding assigned loss factor (η_{rr}) for the satellite oscillators as a function of the normalized index $(\overline{r})$, respectively. (*)

c.1 and c.2. As in Fig. 2a, except that $(\overline{m}_c)$ is changed from (0) to (0.75).

a.

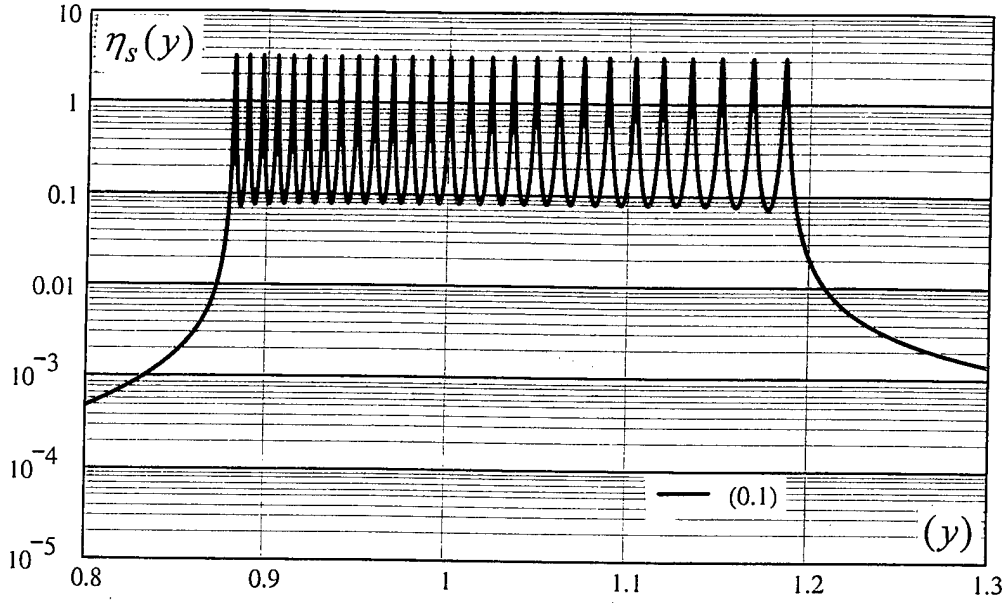

b.

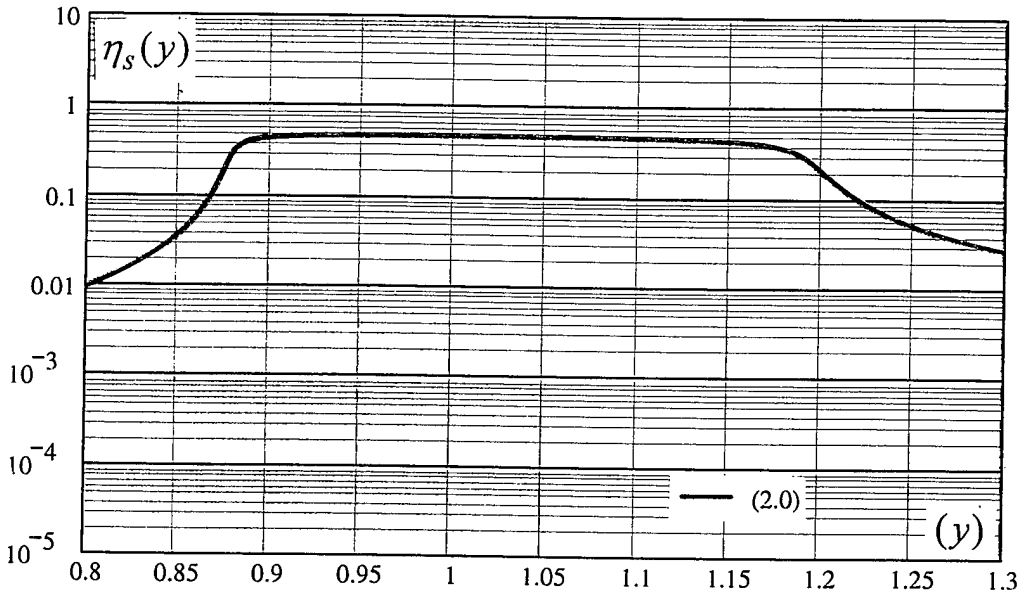

Fig. 3. Induced loss factor $\eta_s(y)\,[=\eta_s^o(y)]$, as a function of (y), for a stiffness control coupling form with α_c =1.0 [α=0.0.], $\overline{g} = \overline{m}_c = 0$. [Sprung-masses.]

a. With b = (0.1)

b. With b = (2.0)

c.

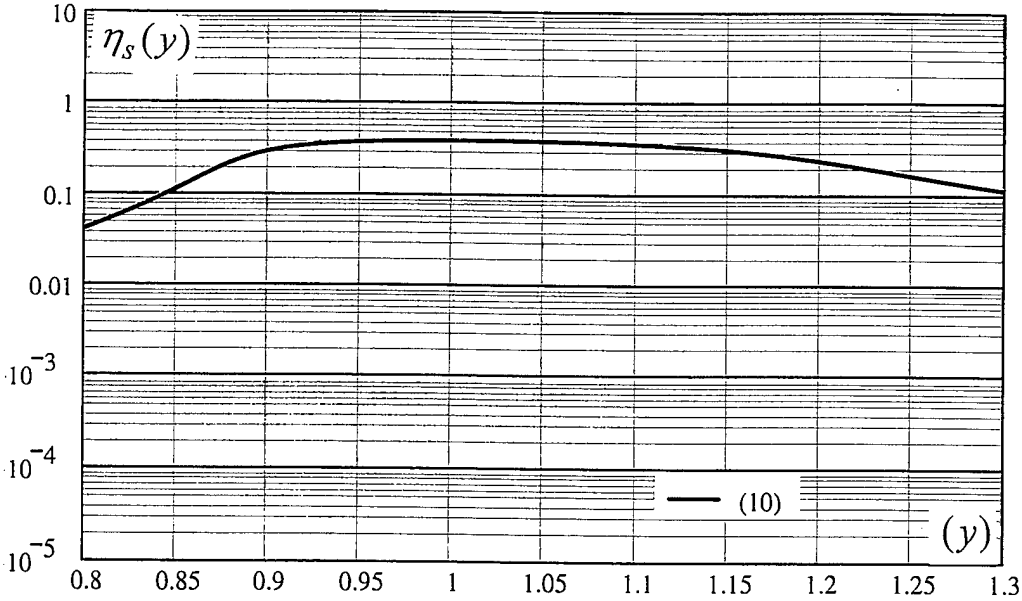

d.

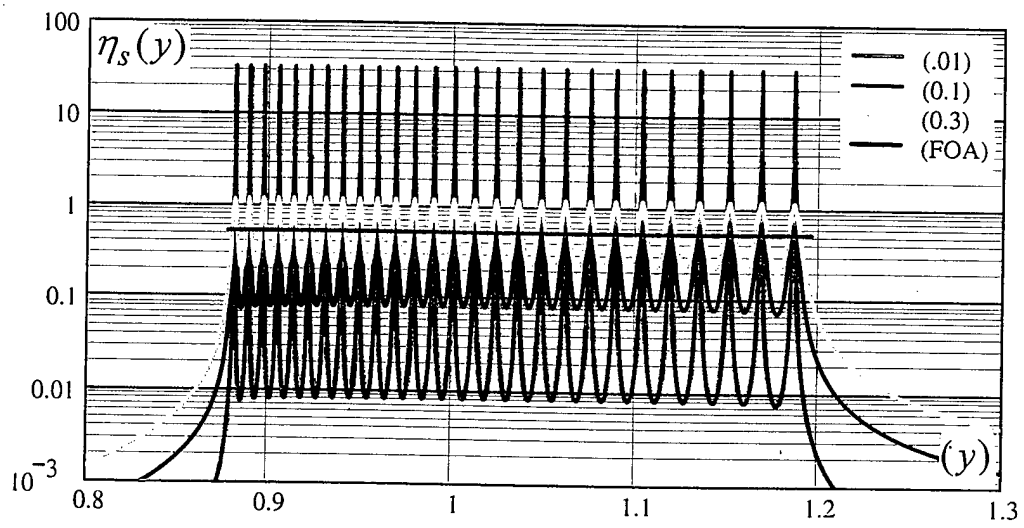

Fig. 3. Induced loss factor $\eta_s(y)$ [$= \eta_s^o(y)$], as a function of (y), for a stiffness control coupling form with $\alpha_c = 1.0$ [$\alpha = 0.0$.], $\bar{g} = \bar{m}_c = 0$. [Sprung-masses.]

c. With $b = (10)$

d. A superimposition of $b = (0.01)$, (0.1) and (0.3), and (FOA). (*)

e.

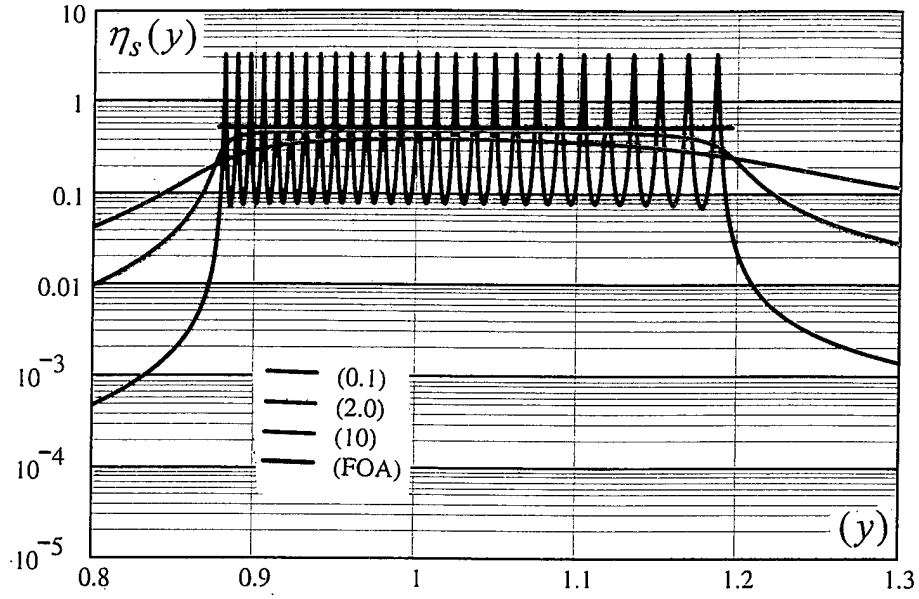

f.

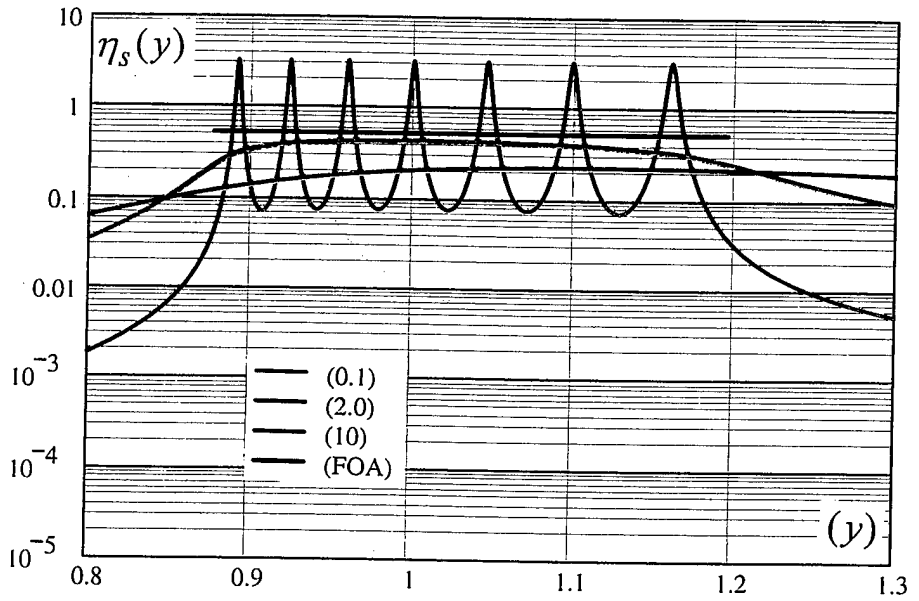

Fig. 3. Induced loss factor $\eta_s(y)\,[=\eta_s^o(y)]$, as a function of (y), for a stiffness control coupling form with $\alpha_c = 1.0\,[\alpha = 0.0.]$, $\bar{g} = \bar{m}_c = 0$. [Sprung-masses.]

e. A superimposition of a, b, and c, and (FOA).

f. As in 3.e above except that R = (7) and not (27).

a.

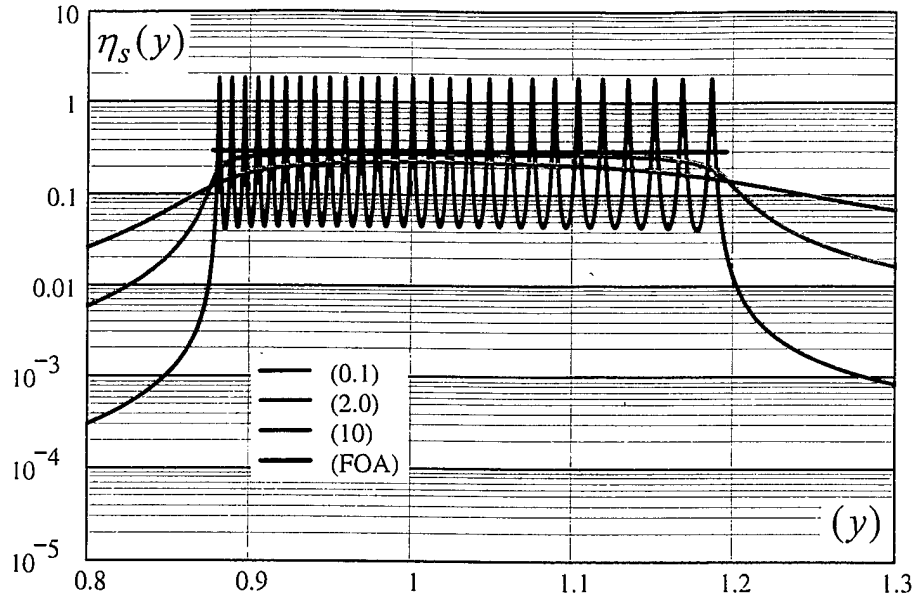

b.

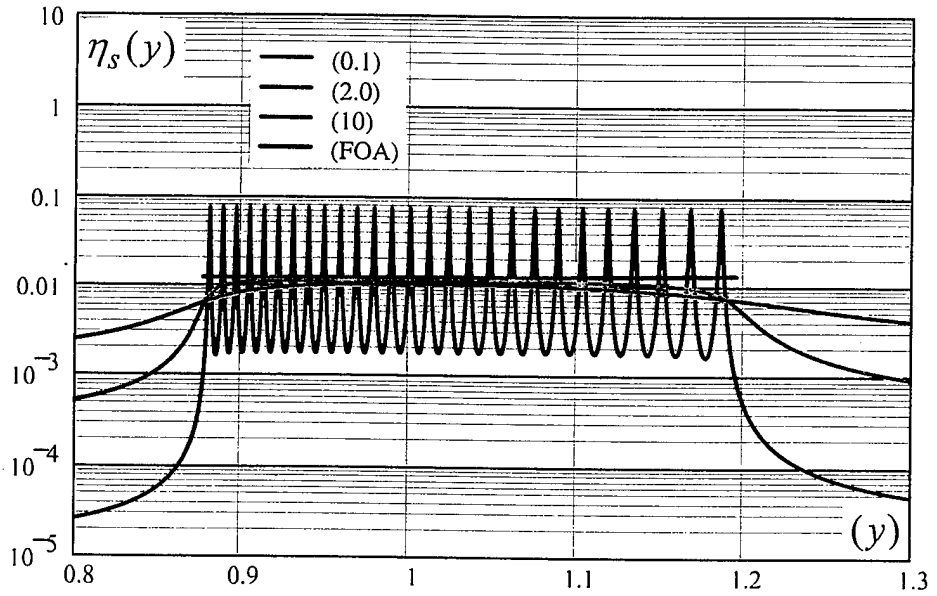

Fig. 4. Induced loss factor $\eta_s(y)$, as a function of (y), for a stiffness control coupling form. [R = 27 and $(M_s/M) = 0.1$.]

a. $\alpha_c = 0.75$ [$\alpha = 0.25$.], $\bar{g} = \bar{m}_c = 0$. [Strong coupling.]

b. $\alpha_c = 0.15$ [$\alpha = 0.85$.], $\bar{g} = \bar{m}_c = 0$. [Moderate coupling.]

a.

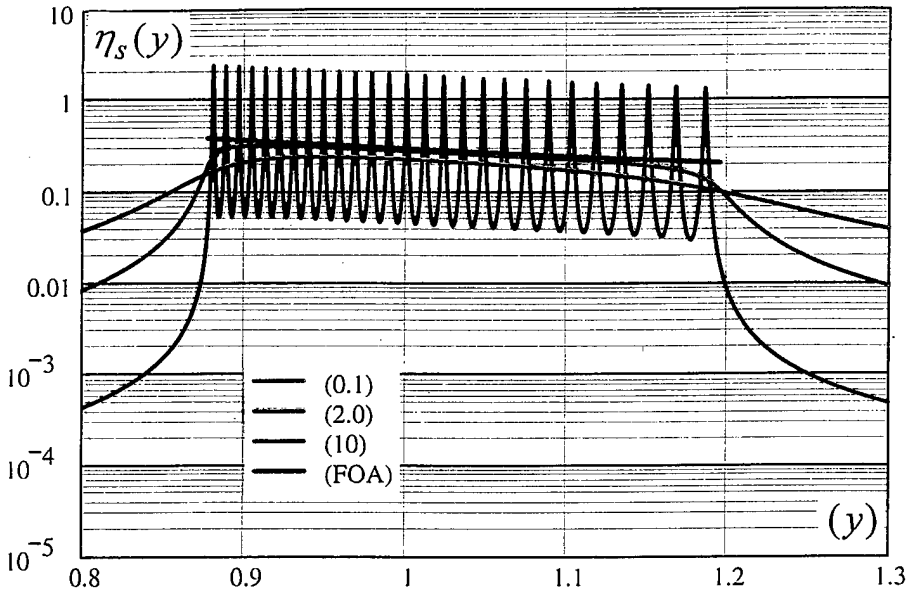

b.

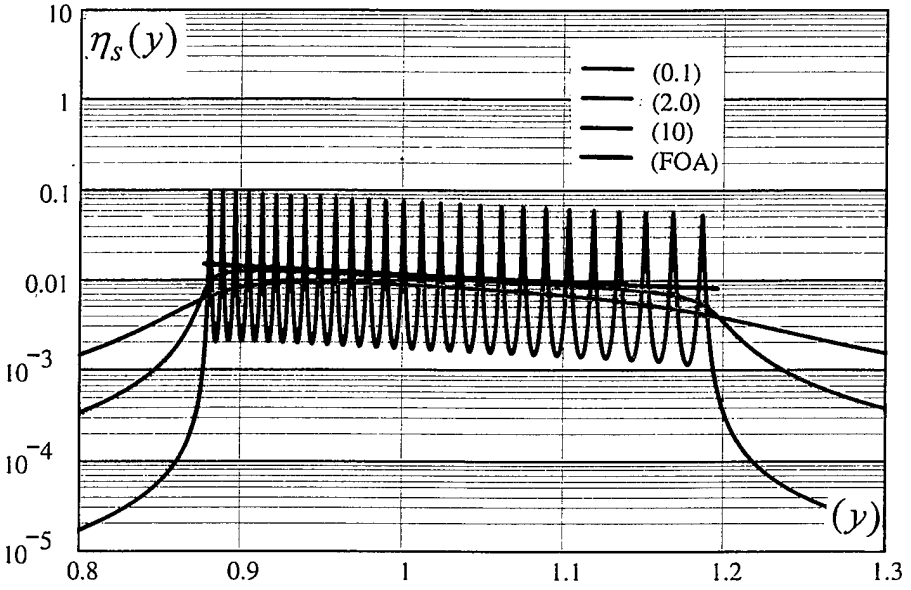

Fig. 5. Induced loss factor $\eta_s(y)$, as a function of (y), for a gyroscopically controlled coupling form. [R = 27 and $(M_s / M) = 0.1$.]

a. $\alpha_c = \bar{m}_c = 0[\alpha = 1.0.]$, $\bar{g} = 0.75$. [Strong coupling.]

b. $\alpha_c = \bar{m}_c = 0[\alpha = 1.0.]$, $\bar{g} = 0.15$. [Moderate coupling.]

a.

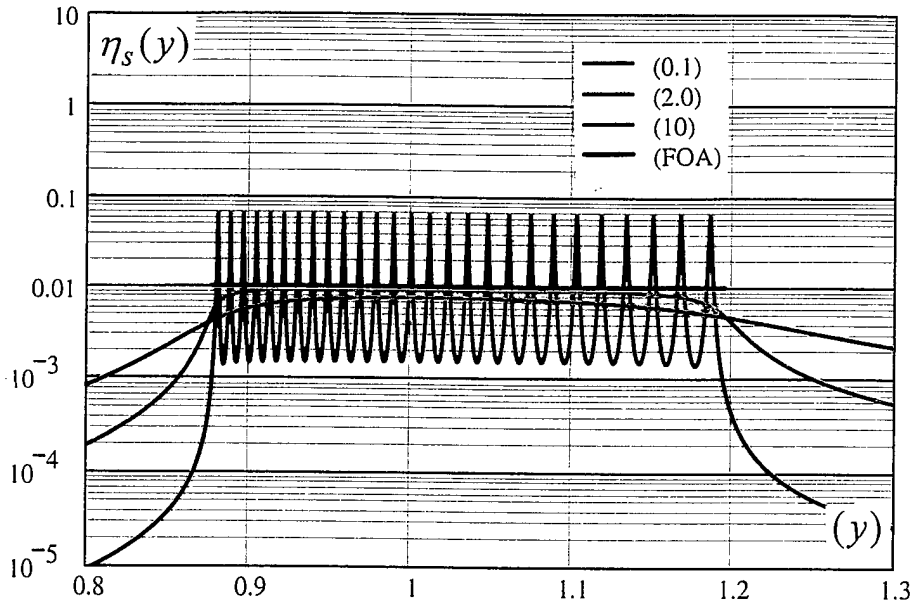

b.

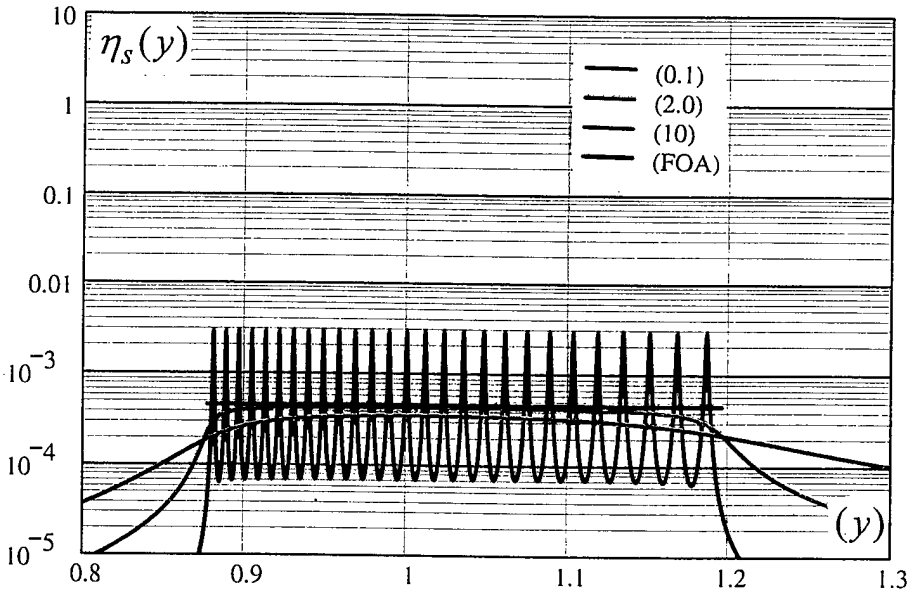

Fig. 6. Induced loss factor $\eta_s(y)$, as a function of (y), for a mass control coupling form. [R = 27 and $(M_s / M) = 0.1$.]

a. $\alpha_c = \bar{g} = 0[\alpha = 1.15.]$, $\bar{m}_c = 0.15$. [Moderate coupling.]

b. $\alpha_c = \bar{g} = 0[\alpha = 1.03.]$, $\bar{m}_c = 0.03$. [Weak coupling.]

a.

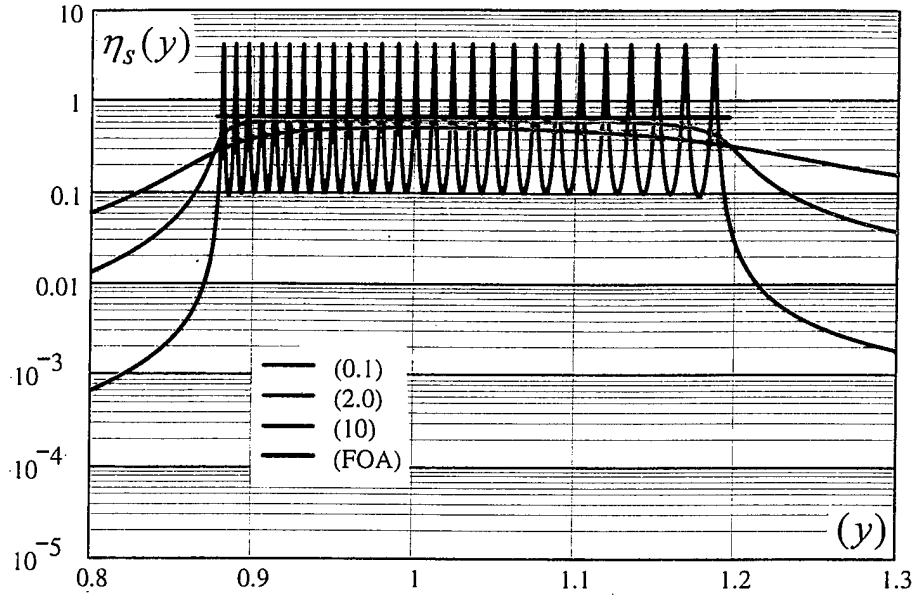

b.

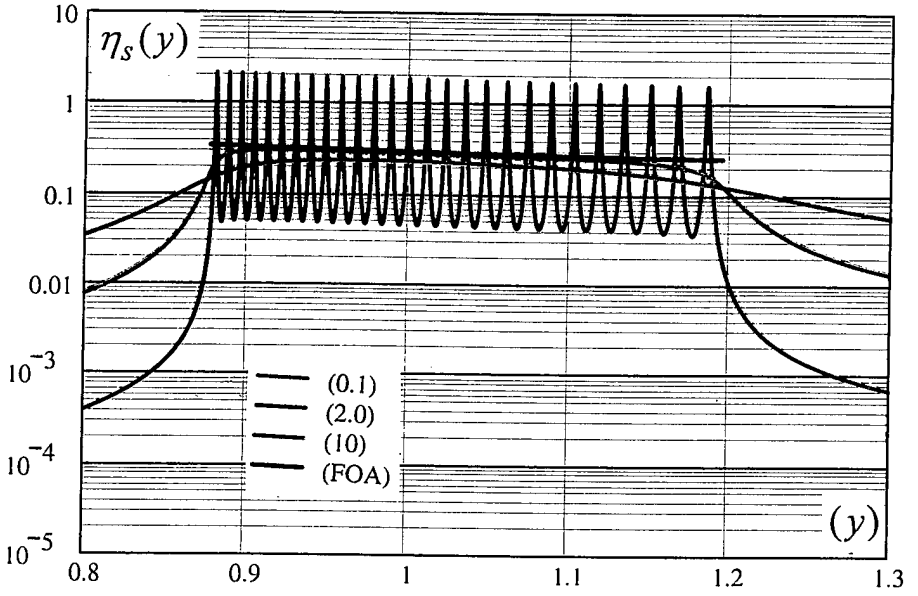

Fig. 7. Induced loss factor $\eta_s(y)$, as a function of (y), for mixed control coupling forms. [R = 27 and $(M_s/M) = 0.1$.]

a. $\alpha_c = \bar{m}_c = 0.75$ [$\alpha = 1.0$.], $\bar{g} = 0$. [Very strong coupling.]

b. $\alpha_c = 0.53$ [$\alpha = 0.47$.], $\bar{g} = 0.54$, $\bar{m}_c = 0$. [Strong coupling.]

c.

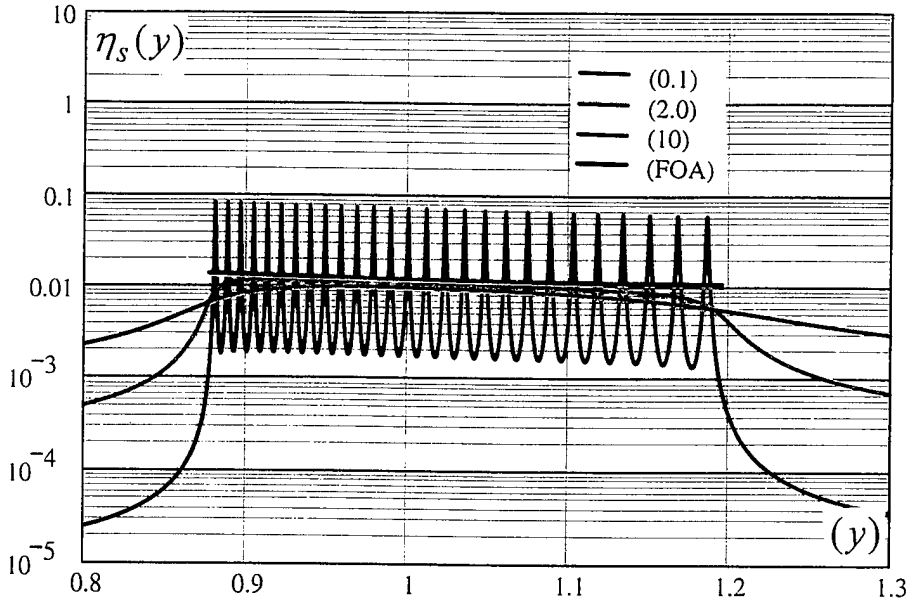

d.

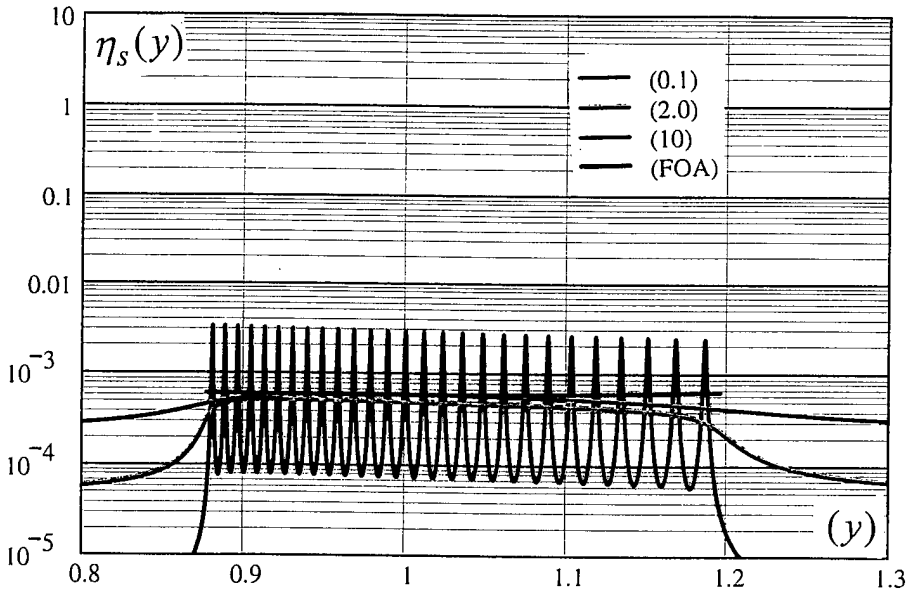

Fig. 7. Induced loss factor $\eta_s(y)$, as a function of (y), for mixed control coupling forms. [R = 27 and $(M_s / M) = 0.1$.]

c. $\alpha_c = 0.10$ [$\alpha = 0.90$.], $\bar{g} = 0.11$, $\bar{m}_c = 0$. [Moderate coupling.]

d. $\alpha_c = 0.02$ [$\alpha = 0.98$.], $\bar{g} = 0.022$, $\bar{m}_c = 0$. [Weak coupling.]

Fig. 8. Pseudo-statistical variations:

a. In the normalized index $\overline{\Lambda}(r)$, as a function of the normalized (integer) index $(\overline{r})$.

b. In the modal overlap parameter (b_r); $(0.1) \le b_r \le (2.0)$.

c. In the modal overlap parameter (b_r); $(1.0) \le b_r \le (3.5)$.

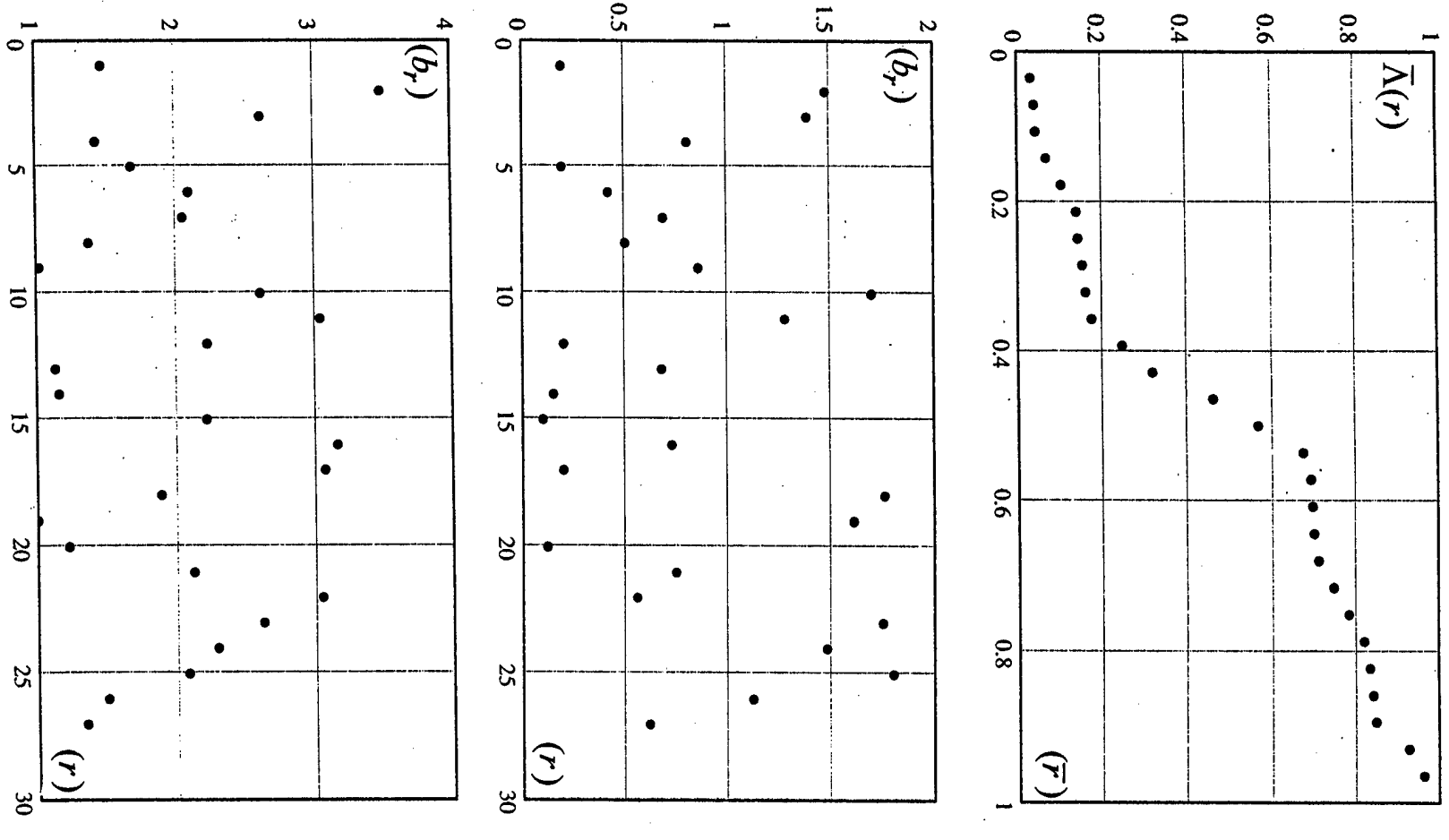

Fig. 9. Modification of pseudo-statistical variations:

a. In the resonance frequency distribution of satellite oscillators, as a function $\overline{\Lambda}(r)$, with $\overline{\Lambda}(r)$ as depicted in Fig. 8a. [cf. Figs. 2a.1 and 2b.1.]

b. In the loss factors assigned to individual satellite oscillators, with (b_r) as depicted in Fig. 8b. [cf. Figs. 2a.2 and 2b.2.]

c. In the loss factors assigned to individual satellite oscillators, with (b_r) as depicted in Fig. 8c. [cf. Figs. 2a.2 and 2b.2.]

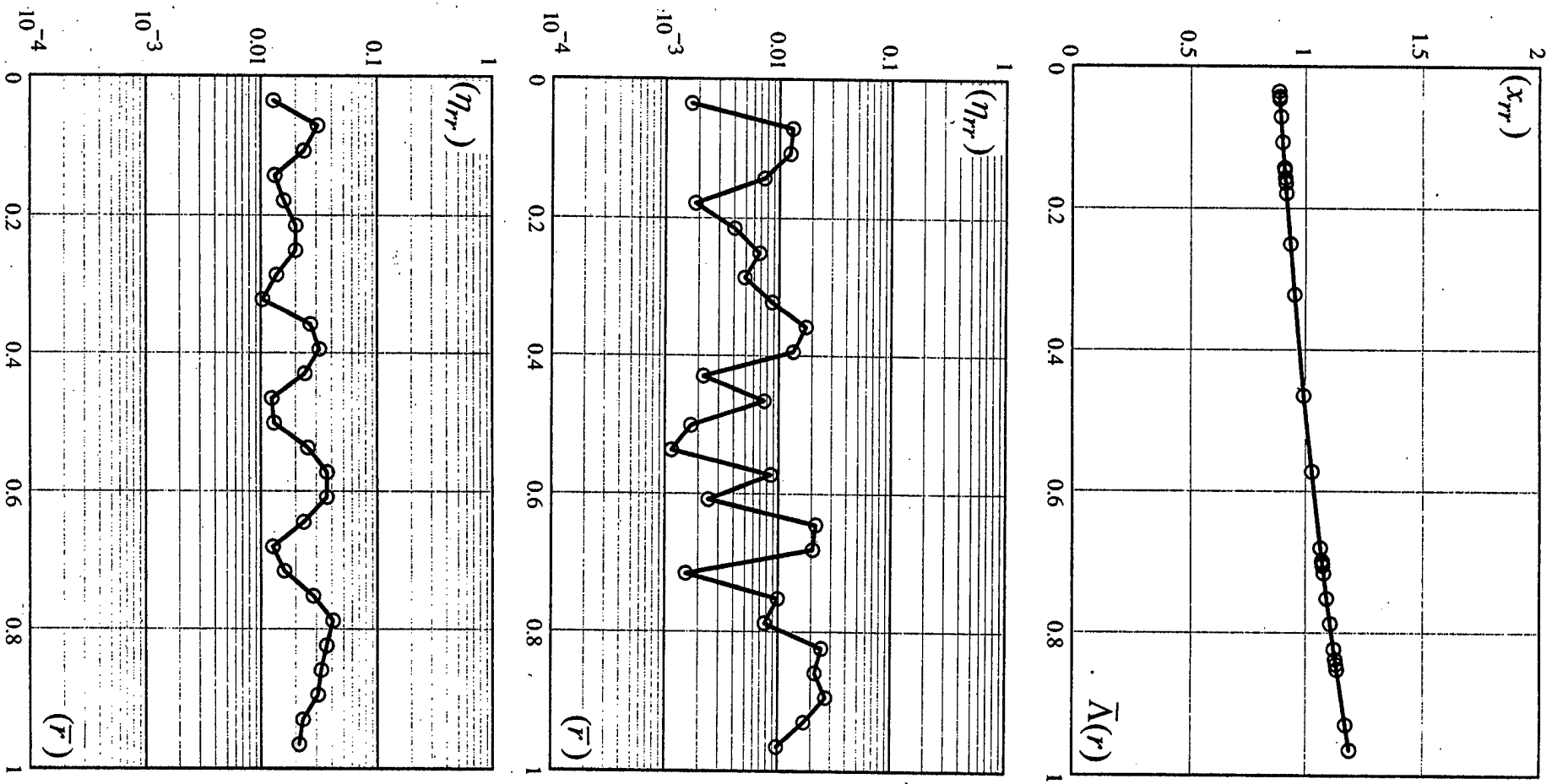

Fig. 10. Induced loss factor $\eta_s(y)$ [$= \eta_s^o(y)$], as a function of (y), for a strong coupling defined by $\alpha_c = 1.0[\alpha = 0.0.]$, $\bar{m}_c = \bar{g} = 0$; implementing a number of pseudo-statistical variations. [R = 27 and $(M_s / M) = 0.1.$] First order approximation is superimposed.

c. $\bar{\Lambda}(r) = \bar{r}$ and (b_r) as is given in Fig. 8b.

b. $\bar{\Lambda}(r)$ as is given in Fig. 8a and $b_r = 1$.

a. $\bar{\Lambda}(r) = \bar{r}$ and $b_r = 1$, a base case.

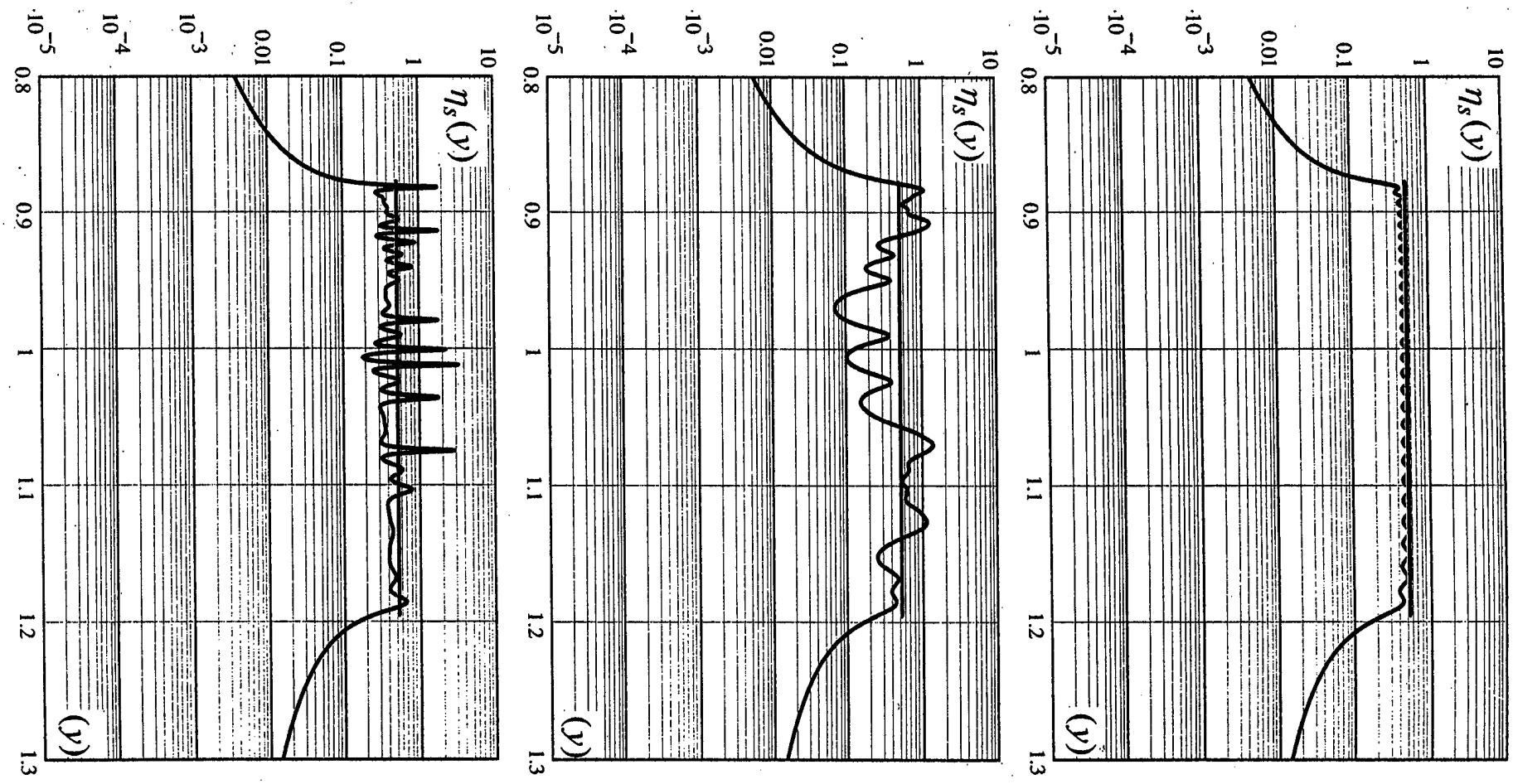

Fig. 10. Induced loss factor $\eta_s(y)\,[=\eta_s^o(y)]$, as a function of (y), for a strong coupling defined by $\alpha_c = 1.0[\alpha = 0.0.]$, $\bar{m}_c = \bar{g} = 0$; implementing a number of pseudo-statistical variations. [R = 27 and $(M_s/M) = 0.1.$] First order approximation is superimposed.

f. $\bar{\Lambda}(r)$ as is given in Fig. 8a and (b_r) as is given in Fig. 8c.

e. $\bar{\Lambda}(r)$ as is given in Fig. 8a and (b_r) as is given in Fig. 8b.

d. $\bar{\Lambda}(r) = \bar{r}$ and (b_r) as is given in Fig. 8c.

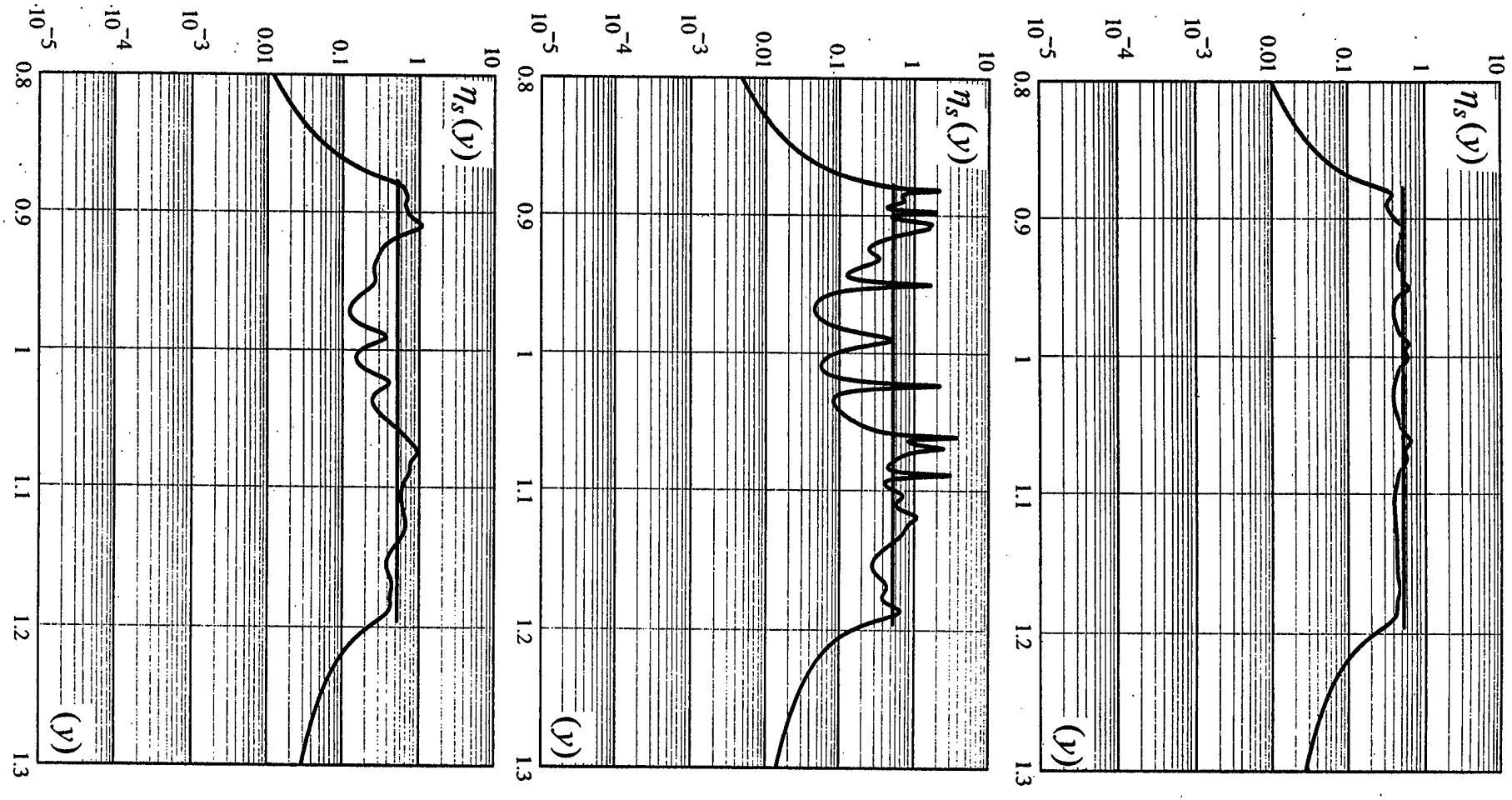

Fig. 11. As in Fig. 10, except that the coupling is a mix of stiffness and gyroscopic control: $\alpha_c = 0.1[\alpha = 0.9.]$, $\bar{g} = 0.11$, $\bar{m}_c = 0$. The coupling strength here is moderate.

a. As in 10a.

b. As in 10b.

c. As in 10c.

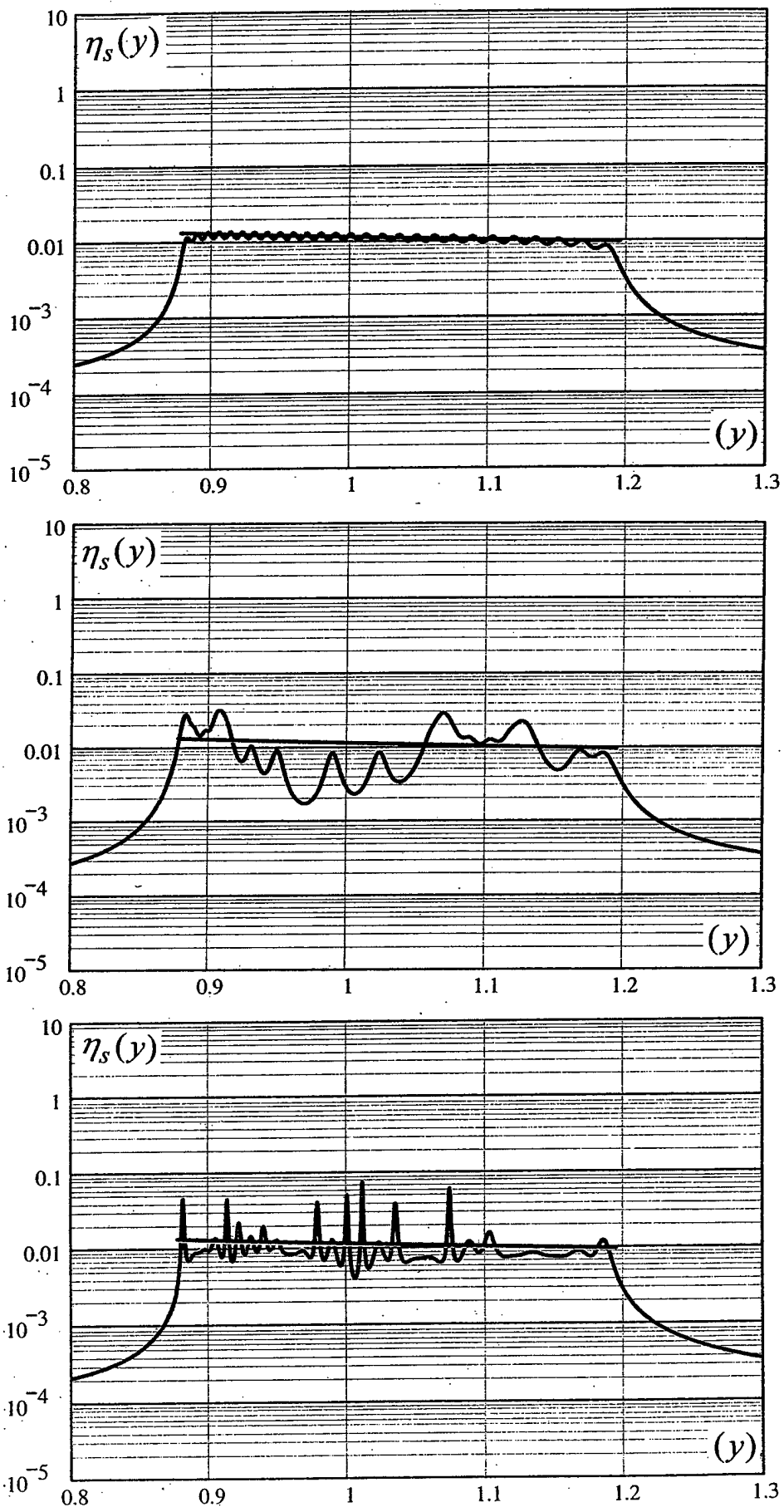

Fig. 11. As in Fig. 10, except that the coupling is a mix of stiffness and gyroscopic control: $\alpha_c = 0.1[\alpha=0.9.]$, $\bar{g} = 0.11$, $\bar{m}_c = 0$. The coupling strength here is moderate.

f. As in 10f.

e. As in 10e.

d. As in 10d.

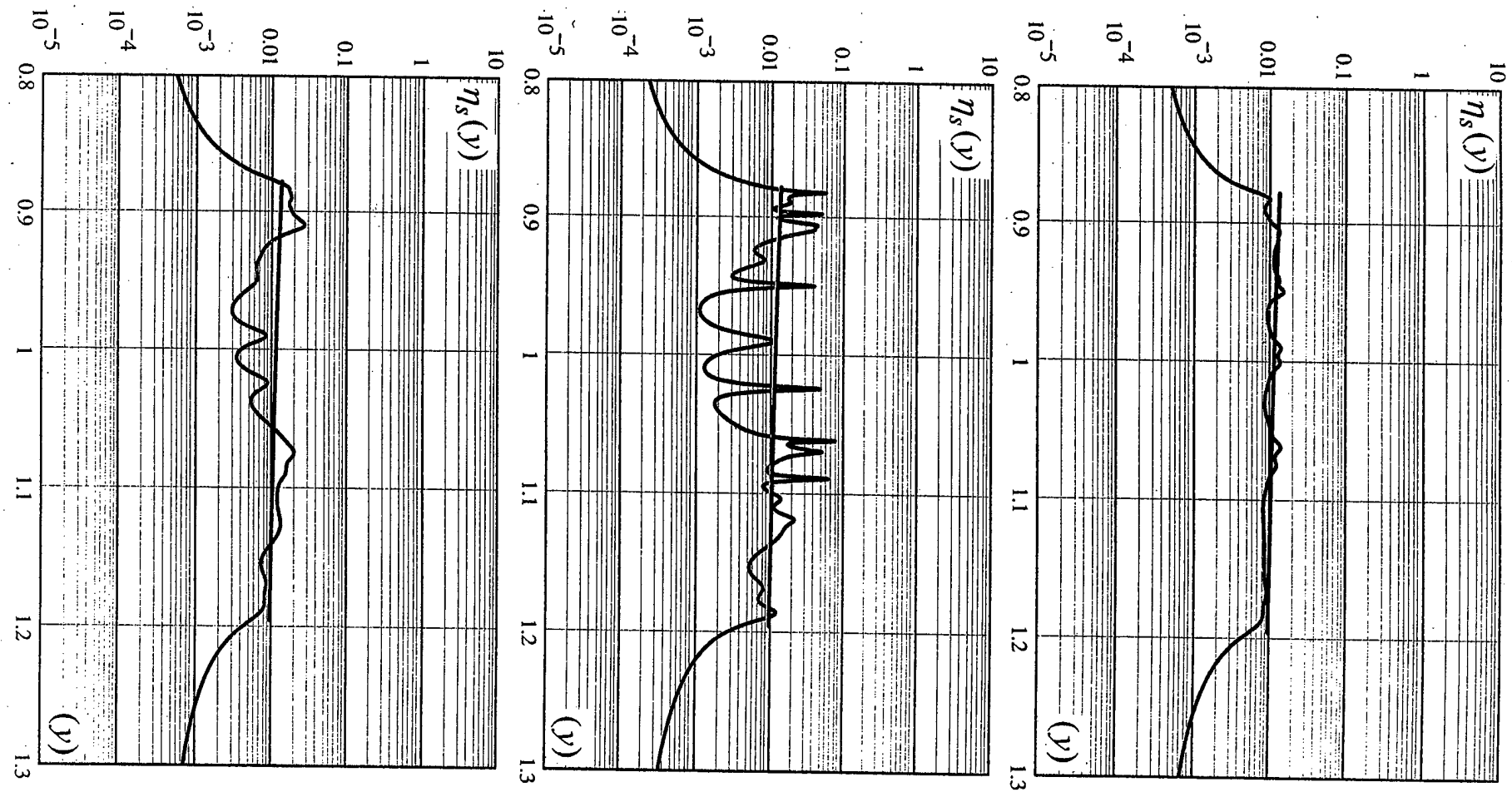

INITIAL DISTRIBUTION

Copies

3 NAVSEA 05T2
- 1 Taddeo
- 1 Biancardi
- 1 Shaw

2 ONR/ONT
- 1 334 Couchman
- 1 Library

2 DTIC

2 Johns Hopkins University
- 1 Green
- 1 Dickey

3 ARL/Penn State University
- 1 Koopman
- 1 Hwang
- 1 Hambric

1 R. H. Lyon, Inc.
- 1 Lyon

1 Cambridge Acoustical Associates
- 1 Garrelick

1 MIT
- 1 Dyer

1 Florida Atlantic University
- 1 Cuschieri

2 Boston University
- 1 Pierce
- 1 Barbone

CENTER DISTRIBUTION

Copies	Code	Name
1	0112	Barkyoumb
1	7000	Dir. Head
1	7014	Fisher
1	7020	Strasberg
1	7030	Maidanik
1	7203	Dlubac
1	7200	Shang
1	7207	Becker
1	7220	Niemiec
2	7250	Maga Diperna
3	3421	(TIC-Carderock)